X-612-65-447

55393

A NEW LOOK AT THE EARTH'S MAGNETIC FIELD

BY

NORMAN F. NESS

NOVEMBER 1965

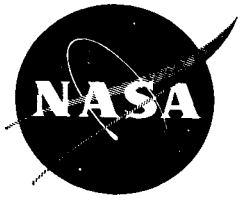

GODDARD SPACE FLIGHT CENTER
GREENBELT, MARYLAND

To be presented at Berkeley, California AAAS meeting "Moving Frontiers in Science" December 26, 1965

A New Look at the Earth's Magnetic Field

Norman F. Ness
Laboratory for Space Sciences
NASA-Goddard Space Flight Center
Greenbelt, Md.

November 1965

To be presented at Berkeley, California AAAS

"Moving Frontiers in Science"

December 26, 1965

A New Look at the Earth's Magnetic Field

Abstract: Satellite experiments reveal that the solar wind confines the geomagnetic field to form the magnetosphere and an extended comet-like magnetic tail.

by

Norman F. Ness

The author is a member of the staff of the Laboratory for Space Sciences, NASA-Goddard Space Flight Center

Table of Contents

A New Look at the Earth's Magnetic Field

Norman F. Ness
Laboratory for Space Sciences
NASA-Goddard Space Flight Center
Greenbelt, Md.

Introduction

Man's early view of the Earth's magnetic field began with the experimental work of men such as Robert Norman, a ship's instrument maker in London. It culminated in the subsequent publication in 1600 by William Gilbert, physician to Queen Elizabeth, of his great treatise de Magnete. These individuals were interested in explaining a terrestrial phenomenon which originated in the ancient curiosity of the attractive properties of a lodestone, This phenomenon, developed into the form of a directional compass, provided a means of navigation for commercial and exploratory endeavors. Although Gilbert's early theory of the origin of the geomagnetic field, as represented in Figure 1, has not proved correct, nonetheless his general conclusions on the geometry and character of the geomagnetic field were amazingly accurate. Subsequent advances in the theoretical description of the phenomenon of terrestrial magnetism came through the work of the mathematicians Laplace, Poisson and finally Gauss who in 1838 published a discussion of the mathematical analysis of geomagnetic field observations.

His application of the methods of potential theory and development of spherical harmonic analysis form the corner-stones of modern techniques of studying the geomagnetic field.

While the general spatial properties of the terrestrial field were being observed, characteristic temporal variations of the geomagnetic field had been identified from detailed studies conducted by a number of research investigators. Principally involved in such a study in 1806 was von Humboldt who deduced that there were periods of rapid fluctuation of the entire terrestrial field associated with auroral displays which he described as a "magnetic storm". These subsequently have been related to solar activity, principally solar flares, and the solar activity cycle as measured by a wide class of solar and terrestrial phenomenon.

More than 25 years ago, Chapman and Bartels (2) published a two volume monumental discourse of research studies on the phenomenon of geomagnetism and the magnetic storm. This summarized their results as well as the efforts of previous research workers in this very old field of scientific investigation. It also marked a decline in the interest of physical scientists in studying the geomagnetic field, for modern physics was then beginning to capture the attention of the majority and the most capable research investigators. Continued studies of the

geomagnetic field and its characteristic variations have been carried on by a small number of dedicated workers. The principal results of such studies are surface maps of the geomagnetic field showing the direction, magnitude and rates of change of the terrestrial field. An example of one of the first such maps is shown in Figure 2, representing an "isogonic" map of epoch 1500. Such world-wide maps are maintained currently by the Hydrographic Offices of different countries for use in navigation.

The advent of the satellite and space probe era 8 years ago coupled with a renewed interest in planetary physics has led to a revolution in the study of planetary magnetism as well as the development of an entirely new field of endeavor, space physics. This has had far reaching consequences because of the scientific results obtained and also the large amount of federal funds made available for research related to space activities. This paper will discuss principally results obtained from measurements of the earth's magnetic field by satellites and space probes since 1958. As will become evident from these results, a totally new view of the terrestrial field emerges: one which permits the further development and investigation of many classical problems in geophysics including magnetic storms, aurora, and the

newly discovered radiation belts. In addition it appears that a unique natural laboratory is now available in which to study various phenomenon in the broad field of plasma physics, particularly "collisionless" plasmas.

In a discussion of the phenomenon of geomagnetism there are three areas in which the subject has been investigated and with which this paper could be concerned. Clearly the precise description and quantitative analysis of the present state of the geomagnetic field are of fundamental significance. Equally important however is the history of the geomagnetic field both in recent and ancient times and finally the origin of the geomagnetic field, The origin has escaped and eluded quantitative and explicit theories even with present modern computer capabilities to study such large scale geophysical systems.

This paper, as indicated, is directed towards a brief summary of those satellite experiments providing direct measurements of magnetic fields in space, principally the distant terrestrial field. These data have been obtained from both close orbiting satellites at elevations of only a few hundred kilometers above the Earth's surface to satellites with highly eccentric orbits penetrating more than 2.5×10^6 Kms into interplanetary space. The interpretation of such data depends critically upon the accuracy of the measurements but is relatively straight forward with respect to a description of the magnetic field. However, in an attempt to understand

the physics associated with the current state of the geomagnetic field it is necessary to either directly or indirectly incorporate the effects of the motion of charged particles. Indeed the importance of the geomagnetic field today can be compared to the original motivation for its study more than 300 years ago. At that time navigation of commercial shipping on the oceans of the Earth was of great significance. Today the motion of charged particles as "guided" by the magnetic field in space is the "navigation" property of interest.

A discussion of the external geomagnetic field must of necessity begin not with the Earth but rather with the Sun and the phenomenon of the "solar wind". The configuration of the outer most field lines of the distant geomagnetic field as well as the interplanetary magnetic field is dominated by this solar plasma flux. That the sun would continuously emit an energetic plasma is a property of the interplanetary medium which has only recently been predicted and subsequently measured by satellites.

Conceptually, a solar plasma flux was introduced by Chapman and Ferraro in the early 1930's in their studies of the phenomenon of the magnetic storm (reviewed by Chapman (3)). Following a solar flare, it was postulated that the sun emitted an electrically neutral but ionized "gas"

which interacted with the geomagnetic field. The solar plasma compressed and confined the field temporarily to a region of space referred to as the Chapman-Ferraro geomagnetic cavity. This plasma flow was considered to be a transient feature on the sun and it was not until early in the 1950's that continual emission of substantial solar plasma was seriously considered. Biermann (4), in studying the characteristics of type I comet tails which contain ionized constituents such as CO^+, postulated a continuous and substantial solar corpuscular flux. This was necessary to explain the observed antisolar directed and ionized characteristics of comet tails. In the late 1950's, studies of the expansion of the corona by Parker (5) and Chamberlain (6) proposed different theoretical models whose characteristics were best described as either the solar wind or breeze depending upon the magnitude of the velocity with which the radial plasma flow was predicted. At the present time direct measurements in space have confirmed the solar wind theory as proposed by Parker (summarized in Parker (7)). Figure 3 shows the velocity results for uniform coronal expansion as dependent upon the coronal temperature and radial distance from the sun. It is seen that beyond a few solar radii the solar wind velocity is approximately constant. Direct measurements in space yield velocities in the range $3\text{-}7 \times 10^7$ cms/second (Bridge et al., (8); Snyder and Neugebauer (9)) and densities

in the range 3-70 protons/cc. The concept of the solar wind as a continuous solar plasma flux is important in a study of the present state of the geomagnetic field because of the far reaching effects which result from the interaction of the solar wind with the geomagnetic field.

The Magnetosphere and Its Boundary

The continual flux of solar plasma confines the geomagnetic field to a region of space which is now referred to as the magnetosphere. Less than three years ago Hines (10) presented in this journal a paper on the magnetosphere boundary entitled "The Magnetopause: A New Frontier in Science". Rapid advances in experimental results coupled with theoretical studies have shown that the confined and highly distorted geomagnetic field offers a number of new problems as well as possible solutions to many familiar problems in terrestrial and extra terrestrial physics. Figure 4 presents a simplified illustration of the interaction of the solar wind with the geomagnetic field as suggested in studies prior to 1962. The rarefied solar plasma, consisting principally of protons of approximately 1 KeV energy with approximately 5% helium ions, is shown to interact with the geomagnetic field as a collection of separate particles. The magnetic field turns the particles around, reflecting the plasma flow and an effective electrical current is developed on the boundary. Satellite measurements of the distorted geomagnetic field within the magnetosphere as well as its boundary characteristics have been made since 1958.

These measurements show that as a direct result of the flux of the low energy plasma from the sun and its interaction

with the geomagnetic field, extraterrestrial space can be divided into three characteristic regions:

1. The interplanetary region where the properties of the interplanetary medium are undisturbed by the presence of the earth and its magnetic field,
2. The magnetosheath or interaction region associated with the impact of the solar wind on the geomagnetic field and
3. The magnetosphere, that region of space containing the geomagnetic field and encompassing the earth in the classical concept of the Chapman-Ferraro geomagnetic cavity.

Separating these regions are two surfaces whose physical characteristics have only recently begun to be investigated:

1. The collisionless magnetodydrodynamic shock wave surface separating the undisturbed interplanetary medium from the magnetosheath.and
2. The magnetopause separating the interaction region from the magnetosphere.

This paper will discuss only the magnetosphere and its boundary layer, the magnetosheath. A summary of all satellites and space probes which have carried magnetometers for the explicit purpose of measuring fields in space is given in Table I. Those experiments which have yielded mainly data on the geomagnetic field are

included along with their pertinent spacecraft orbital characteristics and experiment parameters. Projected on the plane of the ecliptic in Figure 5 are the relative positions of these satellite orbits with respect to the earth-sun line. The position of the magnetosphere boundary and the shock wave surface are also shown.

Although early measurements on the Pioneer I and V satellites (11,12) in 1959 suggested termination of the regular geomagnetic field at approximately 14 R_E no continuous traversal of the boundary was observed because of intermittent satellite data transmission. Less than 5 years ago the first experimental evidence on the confinement of the geomagnetic field and observations of its boundary were obtained by the Explorer X satellite magnetic field and plasma experiments of Heppner et al., (13) and Bonetti et al. (14). This satellite, launched in March 1961, transmitted useful information only to apogee of its first orbit. However, these data revealed a large scale distortion of the geomagnetic field on the antisolar side of the earth and an intimate anti-correlation between the solar plasma and the magnitude of the magnetic field.

Earlier detailed mapping of the geomagnetic field close to the earth on the Explorer VI satellite (15,16) in 1959 had yielded data initially interpreted to indicate the existence of a permanent "ring current", due to charged particles

in regular axially symmetric motion around the Earth at distances of 8-10 R_E. (The magnetic field of such a current system is directed opposite to the Earth's field at distances $< 8\ R_E$ and parallel with the geomagnetic field at distances $> 10\ R_E$). However these measurements yielded only a component of the field and not the complete vector so that a unique interpretation was impossible. Subsequently the Explorer VI data were reexamined and shown to be consistent with the general distortion of the geomagnetic field as indicated by Explorer X and later satellite measurements (17). Russian measurements of the distant terrestrial magnetic field on the moon probes Luniks I and II detected large depressions of the main field at 2.8-4.0 R_E (18,19). Recently the Russian Electron 2 earth satellite (20) has also confirmed in approximately the same region of space smaller depressions of the field than those observed on previous USSR launches. Direct particle measurements in the radiation belt (21) do not reveal the existence of particle fluxes adequate to explain the magnetic field data in terms of a ring current. The magnetic field data must be interpreted in terms of a permanent non-axially symmetric distortion of the magnetosphere so that the local time of data observations must be considered.

Shortly after Explorer X, the US launched the Explorer XII satellite in August 1961, the first in a series of increasingly sophisticated satellites to investigate various particle, field and plasma phenomenon in the geomagnetic field and interplanetary space. These measurements (22,23) showed a termination of the compressed geomagnetic field at a distance between 8-10 R_E on the sunlit side of the earth and simultaneous termination of the Van Allen trapping region for energetic particles. In addition, an increased plasma flux, inferred to be thermalized solar plasma, was also observed beyond the magnetosphere. These particle and field measurements, combined with the Explorer X data, established experimentally the permanent existence of a confined and compressed geomagnetic field.

The relative positions of the magnetosphere and its boundary layer as measured by the Explorer XII satellite are shown in Figure 6. These data are projected on the equatorial plane of the earth and show the roughly spherical shape of the magnetosphere boundary near the subsolar point and also the limited extent of the thermalized plasma. It was also possible with these direct measurements of the boundary position to place in a proper perspective the earlier measurements by the Pioneer and Explorer satellites (25).

A comprehensive survey of the confined geomagnetic field, its boundary and significantly magnetic measurements at the collisionless shock wave have been made by the Explorer XVIII (IMP-I) satellite (26,27). The magnetic field measurements, as presented in the solar ecliptic coordinate system,+ are shown in Figure 7 on the orbit that passed nearest to the subsolar point on the magnetosphere boundary.

It is seen that the observed magnetic field within the magnetosphere (< 10.8) R_E is directed parallel

+ Footnote:

In a study of the interaction of the solar wind with the geomagnetic field, a coordinate system has been introducted which reflects the importance of the solar origin of the plasma. Direct measurements of the solar wind indicate velocities between 3-7 x 10^7 cm/sec. The heliocentric orbital motion of the earth through interplanetary space is only 3 x 10^6 cm/second so that the direction of the solar plasma flow is aberrated from the sun-earth-line by only 3 to 6 degrees. A right handed geocentric solar ecliptic coordinate system comprising an X_{se} axis directed from the earth to the sun and the Z_{se} axis normal to the ecliptic plane has been found to be a useful reference in which to study measurements of fields and plasmas. In this coordinate frame, θ is the latitude and Φ the longitude as measured East of the Sun.

to that theoretically predicted. The magnitude of the field is increased abruptly within the magnetosphere boundary and gradually approaches the theoretical value near the earth. The disturbed character of the magnetic field and rapid fluctuations observed beyond the magnetosphere boundary are typical of observations within this particular region of space. Plasma measurements obtained by the same IMP-I satellite (8) have shown a remarkable correlation with the position of the magnetosphere boundary. The existence of an approximately isotropically directed flow of plasma immediately beyond the boundary is generally observed.

It is noted that the magnitude of the field at the magnetosphere boundary is approximately twice that which would be due to the earth's field alone. This is understood by considering the diamagnetic effects of the plasma which must compress and thereby exclude the terrestrial magnetic field so that the normal component at the boundary is zero. An image dipole on the solar side of the magnetopause with the same value as the Earth's will yield a zero normal component at a plane boundary approximating the magnetopause. At the boundary it will lead to a doubling of the field magnitude. More detailed computations of the shape of the magnetosphere boundary have been conducted by a number of investigators, as summarized by Beard (28). In general they employ the simplified model shown in Figure 4.

There has been some discussion about the appropriate physical character of the reflection of plasma at the boundary. but the results are mutually in good agreement. The mathematical problem solved is one in which the boundary conditions are known but the position of the boundary is to be deduced. This represents a variation to the classical boundary value problems which are familiar in mathematical physics.

It is possible to estimate the distance at which the geomagnetic field will terminate by consideration of the balance of magnetic pressure and plasma momentum flux at the subsolar point.

Let B_o = the equatorial field strength of the earth

n = the plasma density

V_s = the solar wind velocity

B_b = the total field at the magnetosphere boundary

and R_b = the geocentric radial distance to the magnetosphere boundary

then pressure $= 2mnV_s^2 = B_b^2/8\pi$

but $B_b = 2B_o (R_E/R_b)^3$

thus $R_b = R_E \left[B_o^2/4\pi mnV_s^2\right]^{1/6}$.

Substituting B_o = 0.312 Gauss, n = 2-10 protons/cc and V_s = 4×10^7 cm/second yields R_b = 8-11 R_E which is in reasonably good agreement with observations.

The magnetic field measurements obtained on outbound IMP-I orbit #1 at an angle of 45^{o} to the sun-earth-line are shown in Figure 8. As before it is seen that the magnitude of the field is above that theoretically predicted within the magnetosphere and that at 11.3 R_E an abrupt decrease occurs in the magnitude as the directional character of the field changes to rapidly fluctuating. Higher frequency fluctuations are inferred from the separate presentation of the individual X_{se} - Y_{se}-Z_{se} component RMS deviations of the field. At a distance of 16.8 R_E the average magnitude of the field approaches 5 gammas and the directional character of the field stabilizes at the same time the high frequency fluctuations are observed to disappear. This change in character of the field is identified as representing the detached bow shock wave which develops in the supersonic flow of the solar wind as it interacts with the geomagnetic field (29, 30).

The interplanetary medium contains an average magnetic field of approximately 5 gammas (27) and a rarefied density of a few protons/cc so that the phase velocities in the plasma, i.e., the Alfven velocities, are approximately 5 x 10^{6} cm/second. Since the solar wind flow is both deduced (31) and measured

(8,9) to be at least 3 x 10^7 cm/sec, the corresponding Alfvén Mach number of the flow is at least 6 or higher. The characteristic feature of the magnetic field as illustrated in Figure 8 in which the three regions of space defined at the beginning of the paper are so clearly identified is in general observed clearly in each radial traversal of the geomagnetic field while the satellite is passing on the sunlight side of the earth.

Present interpretations of the phenomenon of the solar wind interaction with the geomagnetic field are based upon an analogy with hypersonic gas dynamics. An excellent review of the arguments for this analogy have been presented by Levy, Petschek and Siscoe (32). For reference Figure 9 shows the photograph of a sphere interacting in a hypersonic gas flow at Mach number 14. The shadowgraph shows the development of a discontinuous change in physical properties along the roughly parabolic surface as indicated by the heavy line enclosing this sphere. It is important to recognize that it is not the earth but rather the Earth's magnetosphere which represents a blunt object (approximately spherical on the sunlit hemisphere portion) and which interacts with the solar wind flow to develop the detached bow shock wave.

A direct comparison of the theoretical shape and position of the shock with observations is shown in Figure 10. In this presentation the positions of the shock and magnetosphere boundary are represented by dots and crosses respectively. The solid lines which pass through the dots and crosses represent the theoretical prediction (33) for both the magnetosphere boundary and also the detached bow shock wave. A slight adjustment of the theoretical standoff ratio (measuring the thickness of the magnetosheath) has been made to provide a better agreement between observations and theory. In the gas dynamic analogy this means increasing the equivalent specific heat ratio above the assumed value of 5/3.

At the present time several studies of the precise mechanism leading to the development of a collisionless shock wave with specific application to the case of the solar wind interaction with the geomagnetic field have been conducted (34,35,36). Although the details are not well understood, the observational evidence strongly suggests the existence of a shock wave or at least a shock-like phenomenon in which the characteristics of the solar wind and the interplanetary magnetic field abruptly change upon penetrating the magnetosheath. The magnetic field is increased and becomes turbulent and the directed solar plasma flow is randomized and the spectrum broadened.

The gross physical characteristics at the boundary of the magnetosphere have been measured by a number of satellite experiments. An important finding of the measurements has been the extreme narrowness of the magnetosphere boundary. With the assumption of a fixed position of the boundary during a satellite traversal, it is found that the thickness of the magnetopause is a very small fraction of an earth radius, $\pm 2 \times 10^7$ cms. Levy et al (32) have analyzed the problem of the detailed characteristics of the magnetopause boundary layer surrounding the magnetosphere, as shown in Figure 11. They consider the magnetopause as an Alfvén wave and a slow expansion wave which are coincident near the subsolar point but which separate near the polar regions. In addition, as originally noted by Dungey (37), there is every reason to anticipate a connection of high latitude geomagnetic field lines to the interplanetary magnetic field as shown in Figure 11. This connection of field lines has further implications for the configuration of the field on the night side of the earth. Satellite measurements at present are not sufficiently definitive to ascertain if the model as proposed is valid and indeed to what extent connection exists on the sunlit hemisphere of the magnetosphere.

The Earth's Magnetic Tail

In a 1960 study of the phenomenon of the geomagnetic storm, Piddington (38) suggested that magnetic field lines would temporarily be extended on the nightside of the earth somewhat as shown in Figure 12, distorted by an effective viscous stress of the solar wind on the outermost lines of force. The first measurements of the earth's magnetic field on the night side of the Earth at great distance by Explorer X in 1961 indicated that such a distortion existed even in the absence of a geomagnetic storm. Subsequently Explorer XIV (40) revealed near local midnight an apparent electron "tail" in the energetic particle distribution as shown in Figure 13. On the same satellite Cahill (41) measured the terrestrial field approaching approximately an antisolar direction at a distance of 16 R_E. Recent detailed experimental measurements mapping the earth's magnetic field on the nightside of the Earth performed by the IMP-I satellite (42) have shown that the geomagnetic field trails out far behind the earth at least halfway to the moon and forms a substantial and permanent magnetic tail.

That such an appendage to the geomagnetic field would exist permanently had been recently predicted (39, 43, 44, 45). A magnetically neutral region separating oppositely directed fields has been detected (42) and is illustrated as the neutral plane in Figure 12. In the model of Dessler (43,44) the earth's magnetic field trails out far behind the

earth to 20-50 A.U. (astronomical unit) following the flow of plasma from the Sun with negligible merging of field lines across the neutral plane from the upper and lower regions of the tail. An alternative view has been taken by Axford et al. (45) based upon initial suggestions by Dungey (37) in which an appreciable merging of field lines on the nightside of the earth would lead to the development of a neutral line and sheet region which would contain enhanced particle fluxes, such as those observed by Explorer XIV.

Detailed measurements from the IMP-I satellite on orbit #41 in May 1964 yielded data obtained when the satellite was closest to the midnight meridian plane (Figure 14). Inspection of this data demonstrates the remarkable feature of the direction of the field paralleling closely the Earth - Sun-line ($\theta = 0^{o}$ and $\Phi = 0^{o}$ or 180^{o}) and directed either toward ($\Phi = 0^{o}$) or away ($\Phi = 180^{o}$) from the Sun depending upon whether the satellite is above or below the magnetically neutral region identified as the neutral sheet. Shown in Figure 14 on the inbound portion of the orbit is the abrupt change in the direction of the magnetic field at 16 R_E. Although the satellite motion is

predominately radial there is also a slight transverse motion so that the apparent thickness of the transition across the neutral sheet implies an extremely thin feature in the earth's magnetic tail.

A summary of the IMP-I observation of the earth's magnetic tail is presented in Figure 15 showing the XY components of the magnetic field projected on the ecliptic plane. This presentation, with little distortion, presents a correct view of the geomagnetic tail field. These data are separated to show the results obtained when the satellite is above or below an imaginary plane at 2.5 R_E below the ecliptic (chosen for clarity of presentation). In this figure it is possible to follow the individual satellite orbits and identify a single or indeed multiple traversal of the neutral sheet on each orbit. Multiple traversals of the neutral sheet are interpretable in view of the "wobble" of the earth's magnetic dipole axis once every 24 hours and the associated orientation of the magnetic neutral sheet (42).

The general interpretation ascribed to the observations is that lines of force originating in the polar cap regions of the earth are distorted by the solar wind to trail out far behind the earth and form the magnetic tail (see figure 16). On this basis it is possible to predict the colatitude of the polar cap region which will correspond to the observed characteristics of the magnetic tail field.

Let R_T = radius of tail

B_T = tail field magnitude

θ_{pc} = colatitude of polar cap region

then conservation of flux or connection of field lines between the polar cap and the tail requires that

$$B_T = 4B_0 (R_E/R_T)^2 \sin^2 \theta_{pc}$$

Substituting a value of 16 gammas obtained from the IMP-I measurement for the median magnitude of the field in the earth's tail (46) and an approximate radius of the earth's tail of 22 R_E (42) yields a predicted polar cap region of approximately 18^o co-latitude. This corresponds well with the polar cap region defined by the auroral zone and also the boundaries of the trapped radiation belts. The observations of the radiation belt have shown that there is a strong day-night asymmetry in the invariant latitude at which the trapped particles are observed to terminate so that the distortion suggested as in Figure 12 is substantiated by experimental data. Measurements of intense particle fluxes at higher latitudes than the radiation belts (47) suggest that their origin is within the geomagnetic tail. At the present time it appears plausible that the

tail is the source of these energetic particles which form the aurora (48). However the exact mechanisms for acceleration of solar plasma particles to auroral energies is not clear.

Magnetic Storms

The theoretical study of magnetic storm phenomenon originally led to the suggestion of the transient flux of plasma from the sun compressing the geomagnetic field and leading to the initial increase in the horizontal component of the geomagnetic field (2). Subsequently the solar particles were trapped in the geomagnetic field in a "ring current" which then led to the classical main phase decrease of the terrestrial field for a day or so afterwards. The decay of this ring current then occurred and the geomagnetic field resumed its normal configuration. With the recent measurements of a continual plasma confinement of the geomagnetic field and the permanent existence of the earth's magnetic tail, revisions of these concepts are necessary in order to analyze the magnetic storm phenomenon.

Several magnetic storms occurred during the lifetime of the IMP-I satellite while measurements were being performed in the magnetic tail. One on May 10 has the classical characteristic observable in the ground station records of an initial sudden increase in the horizontal component followed by a decrease and recovery over a time scale of several days (see Figure 17). Correlated with these data in this figure are the magnetic field measurements obtained in the earth's magnetic tail. It is seen that the sudden compression of the magnetosphere, associated possibly with a propagating shock wave in the interplanetary medium,

is observed at 0035 UT on May 10. The correlation and anti-correlation of magnetic field variations in the tail with those on the earth's surface correspond to changes in pressure and tension on the distant lines of force of the magnetic field (49).

In Figure 18 measurements of the boundary of the trapping region are compared with measurements of the earth's magnetic tail field during a magnetic storm in April, 1964. Satellite measurements of the trapping boundary at an elevation of 1000 Kms were performed by the APL satellite 1963-38C. Prediction of the termination of the trapping boundary invariant latitude is obtained utilizing a theoretical model of the distorted geomagnetic field which includes a tail and neutral sheet. Although there exists a discrepancy in the observed and predicted position of the trapping boundary for the particle energies observed, the changes in this boundary are seen to be coincident in time and equal in magnitude with theory. This lends very strong support to this tail field topology. In addition Kp is noted to be correlated with the tail field magnitude. Detailed studies of the tail field (46) during a three month period have indicated that Kp is generally positively correlated with tail field magnitude and indicate that an increase of solar plasma flux drags additional lines of force into the Earth's magnetic tail.

Summary

This paper has presented experimental results obtained from mapping the earth's magnetic field during the past eight years with the most unique "laboratory benches" yet developed: satellites and space probes. They have introduced and stimulated considerable activity in the new field of space physics. They have also brought to many classical geophysical problems a clear, fresh and more accurate insight. This is particularly true in the field of geomagnetism in which the earth's magnetic field is now known to be continuously compressed by a solar corpuscular flux, the solar wind, and terminated at approximately 65,000 kilometers towards the sun. However, the earth's magnetic field is observed to be extended far behind the earth forming a magnetic tail in an antisolar direction. No termination of the tail at distances more than halfway to the moon is indicated. Suggested tail lengths vary from extremes of 50 A.U. to only 1,000 R_E. In a related experiment the Mariner IV space probe reports the absence of electron fluxes associated with the magnetospheric tail or wake at distances of 3,000 R_E (50). At what distance the tail terminates and what is the character of the termination are problems whose answers are of great significance with respect to our study of the geomagnetic field and related terrestrial phenomenon.

Because of the similiarity of the source phenomenon responsible for the development of this magnetic tail feature it has been noted that the earth may be compared to a "magnetic comet" (see Figure 19). In this context the nucleus of a comet would correspond with the earth, the coma with the magnetosphere and the ionized gas tail with the earth's magnetic tail. Such a suggestion is admittedly rather descriptive although future experimental and theoretical investigations may indicate a substantially more proper and complete analogy. One of the principal problems in the analogy is that there is no known mechansim for producing a large magnetic field in the comet nucleus or coma so the mechanism of formation of the ionized gas tails is not yet clear. The capture of the interplanetary magnetic field offers the most plausible hypothesis at present.

There are two other aspects of the earth's magnetic field which have not been treated but which contribute significantly to a new view of the terrestrial magnetic field. One is the recent result obtained from the Mariner II (51) and IV (52) space probes investigating the magnetic field of the planets Venus and Mars. Although these space probes did not impact the planet, they passed sufficiently close and contained sufficiently sensitive magnetometers and energetic particle detectors that they were able to estimate the strength of these planetary magnetic fields. Compared with the Earth's

magnetic moment of 8×10^{25} emu units, the maximum moment of Venus is only 3.4% and in the case of Mars 0.03%. Thus the Earth is unique among these planets in having such a strong field.

Any mechanism for the origin of the earth's magnetic field must rely principally upon the present geometry and state of the earth and its core. The classical theory of the geomagnetic field origin in a fluid core "dynamo" is still attractive (53). The recent theory of Malkus (54) is particularly pertinent since it depends upon an interaction of the fluid core with the solid mantle and the associated precessional torques. This is significant since the second aspect of recent observations pertinent to our study of the geomagnetic field has occurred in paleomagnetic research on the ancient history of the geomagnetic field. Measurements of the remanent magnetism of rocks show that the direction of the ancient geomagnetic field has been both approximately parallel to and opposite to the present direction of the field (55). This implies that the earth's field has reversed itself. These reversed magnetizations are an important feature of the earth's magnetic field in past times with transitions from one "polarity" to the other observed to occur over relatively short time scales.

This paleomagnetic research coupled with satellite measurements of both the present state of the earth's magnetic

field and data on the absence of magnetic fields on the planets Venus and Mars clearly stimulate future research on the very unique combination of parameters which lead to the existence of the terrestrial magnetic field. The changes in polarity imply a dynamic origin and the existence of the solar wind leads to temporal variations depending upon both the field strength and direction as well as the solar wind flux. Certainly these new experimental results, when fully analyzed and incorporated into theoretical models, will make an important contribution to our concept of the origin of the solar system as it is currently configured.

References

1. J. H. Nelson, L. Hurwitz and D.G.Knapp, Magnetism of the Earth, US Dept. of Commerce Publication 40-1, (1962).
2. S. Chapman and J. Bartels, Geomagnetism Oxford University Press, Oxford, England (1940).
3. S. Chapman, Solar Plasma, Geomagnetism and Aurora, in Geophysics : The Earth's Environment, ed. by C. Dewitt et al. Gordon and Breach N.Y., 373 (1963).
4. L. Biermann, Z Astrophys. 29, 274 (1951).
5. E. N. Parker, Astrophys. J. 128, 664 (1958).
6. J. W. Chamberlain, Astrophys. J. 131, 47 (1960).
7. E. N. Parker, Interplanetary Dynamical Processes, Interscience John Wiley, N.Y. (1963).
8. H. S. Bridge, A. Egidi, A. Lazaruns, E.Lyon and L. Jacobson, Space Research V, 969 (1965).
9. C. W. Snyder and M. Neugebauer, Space Research IV, 89 (1964).
10. C. O. Hines, Science 141, 130 (1963).
11. C. P. Sonett, D.L. Judge, A.R. Sims and J.M. Kelso, J. Geophys. Res. 65, 55 (1960).
12. P. J. Coleman, C.P. Sonett, D.L. Judge and E.J. Smith, J. Geophys. Res. 65, 1856 (1960).
13. J. P. Heppner, N.F. Ness, C.S. Scearce and T.L. Skillman, J. Geophys. Res. 68, 1 (1963).
14. A. Bonetti, H.S. Bridge, A.J. Lazarns, B. Rossi and F. Scherb, J. Geophys. Res. 68, 4017 (1963).
15. E. J. Smith, P.J. Coleman, D.L. Judge and C.P. Sonett, J. Geophys. Res. 65, 1858 (1960).

16. C. P. Sonett, E. J. Smith, D.L. Judge and P. J. Coleman, Phys. Res, Letters, 4, 161 (1960).

17. E. J. Smith, C.P. Sonett and J.W. Dungey, J. Geophys. Res. 69, 2669 (1964).

18. S. Sh. Dolginov, Ye. G. Yeroshenko, L. N. Zhuzgov, N. V. PushKov and L.O. Tyurmina, Art. Earth Sat. 3, 4 and 5, 490 (1960).

19. S. Sh. Dolginov, Ye. G. Yeroshenko, L. N. Zhuzgov, N. V. PushKov and L. O. Tyurmina, Geomag, and Aero. 1, 21 (1961).

20. S. Sh. Dolginov, Ye. G. Yeroshanko and L. N. Zhuzgov, Space Research VI, to appear (1966).

21. R. A. Hoffman and P. A. Bracken, J. Geophys. Res. 70, 3541 (1965).

22. L. J. Cahill and P. J. Amazeen, J. Geophys. Res. 68, 1835 (1963).

23. J. W. Freeman, J. A. Van Allen and L. J. Cahill, J. Geophys. Res. 68, 2121 (1963).

24. J. W. Freeman, J. Geophys. Res. 69, 1691 (1964).

25. L. J. Cahill, in Space Physics ed. by D. P. LeGalley and A. Rosen, John Wiley and Sons New York, 301 (1964).

26. N. F. Ness, C. S. Scearce and J. B. Seek, J. Geophys, Res. 69, 3531 (1964).

27. N. F. Ness, C. S. Scearce, J. B. Seek and J.M. Wilcox, Space Research VI, to appear (1966).

28. D. B. Beard, Rev. Geophys. 2, 335 (1964).

29. W. I. Axford, J. Geophys. Res, 67, 3791 (1962).

30. P. J. Kellogg, J. Geophys. Res. 67, 3805 (1962).

31. N. F. Ness and J. M. Wilcox, Phys. Rev. Letters 13, 461 (1964).

32. R. H. Levy, H. E. Petschek and G.L. Siscoe, AIAA J.2, 2065 (1964).

33. J. R. Spreiter and W. P. Jones, J. Geophys. Res. 68, 3555 (1963).

34. J. G. Corday, J. Geophys. Res. 70, 1278 (1965).

35. P. D. Noerdlinger, J. Geophys. Res. 69, 369 (1964).

36. F. L. Scarf, W. Bernstein and R. W. Fredricks, J. Geophys. Res. 70, 9 (1965).

37. J. W. Dungey, Phys. Rev. Letters 6, 47 (1961).

38. J. H. Piddington, J. Geophys. Res. 65, 93 (1960).

39. J. H. Piddington, Planet. Space Sci. 13, 363 (1965).

40. L. A. Frank, J. Geophys.Res. 70, 1593 (1965).

41. L. J. Cahill, IGY Bulletin 79, 231 (1964).

42. N. F. Ness, J. Geophys. Res. 70, 2989 (1965).

43. A. J. Dessler, J. Geophys Res. 69, 3913 (1964).

44. A. J. Dessler and R. D. Juday, Planet Space Sci. 13, 63 (1965).

45. W. I. Axford, H. E. Petschek and G. L. Siscoe, J. Geophys. Res. 70, 1231 (1965).

46. K. W. Behannon and N. F. Ness, GSFC preprint X-612-65-417 (1965).

47. I. A. McDiarmid and J. R. Burrows, J. Geophys. Res. 70, 3031 (1965).

48. B. J. O'Brien, Science 148, 449 (1965).

49. E. N. Parker, Phys. Fluids 1, 171 (1958).

50. J. A. Van Allen, J. Geophys. Res. 70, 4731 (1965).

51. E. J. Smith, L. Davis Jr., P. J. Coleman and C. P. Sonett, J. Geophys. Res. 70, 1571 (1965).

52. E. J. Smith, L. Davis, P. J. Coleman and D. E. Jones Science 149, 1241 (1965).

53. R. Hide and P. H. Roberts, The Origin of the Main Geomagnetic Field, in Physics and Chemistry of the Earth, ed. by L. H. Aherns et al., vol. 4, Pergamon Press, London 27 (1961).

54. W. V. R. Malkus, J.Geophys. Res. 68, 2871 (1963).

55. A. Cox and R. R. Doell, Paleomagnetism in Advances in Geophysics 8, 221 (1961).

LIST OF FIGURES

4. Naive representation of the interaction of the rarefied solar wind plasma with the geomagnetic field. Direct impact of the plasma, as represented by individual particles, with the magnetic field is shown specularly reflected from the boundary of the geomagnetic field, which is distorted by this plasma flow.
5. Presentation of the trajectories of satellites and space probes, projected on the ecliptic plane, which have sampled the distant terrestrial and cis-lunar magnetic field. Included also are the relative positions of the boundary of the regular geomagnetic field and the detached collisionless bow shock wave (see text). The position of the moon is shown in proper scale in units of Earth Radii (R_E).
6. Energetic particle measurements obtained from the Explorer XII satellite in 1961 by Freeman (23). Indicated are relative positions projected on the earth's equatorial plane of the various regions surrounding the Earth defined by the energetic particle detectors, which include the classical Van Allen radiation belts.
7. Magnetic field measurements of the distant geomagnetic field from IMP-I on inbound orbit #1, November 30, 1963. The abrupt discontinuity in magnitude and direction of field at 10.8 R_E is identified as the magnetosphere boundary. Theoretical values for $\bar{F}$, Φ, θ are shown

as dashed curves.

8. Magnetic field results on outbound orbit #1 from the IMP-I satellite, November 27, 1963. Clearly evident are the magnetosphere boundary at 11.3 R_E and a termination of the rapid fluctuations of the magnetic field at 16.8 R_E, identified as the collisionless shock wave.

9. Rotating mirror shadowgraph of high speed aerodynamic flow (from left) and the detached bow shock wave surrounding a sphere at Mach 14. (Mach number = flow velocity/sonic velocity).

10. Comparison of the IMP-I shock wave and magnetosphere boundary crossings with the gas dynamic shock model of Spreiter and Jones (33) as projected on the ecliptic plane. Their results, shown as solid lines, have been ajusted to match the observed measurements of the standoff ratio. The predicted shape of the shock is seen to be closely matched by the observations.

11. Schematic drawing of magnetic field (solid lines) and plasma flow (dots) in the subsolar region. The flow is decelerated by the bow shock. The magnetosphere boundary is resolved into an Alfvén wave and a slow expansion fan. (Levy et al. (32)).

12. Schematic diagram of the geomagnetic field as distorted by the solar wind showing lines of force in the noon midnight meridian plane. The "open" tail comprises two

bundles of field lines emerging from the polar caps centered at geomagnetic latitudes of about 87^{o} on the midnight meridian. (Piddington (39)).

13. Schematic diagram of the spatial distribution of electrons (Energy > 40 KeV) as obtained from Explorer 14 measurements in 1963 near the midnight meridian plane Frank (40)).

14. Magnetic field measurements of the earth's magnetic tail near the midnight meridian plane by IMP-I on orbit #41 during April 30 through May 4, 1964. The direction of the field is observed to closely parallel the earth-sun line with a rapid change from antisolar to solar directed sense on the inbound pass at a radial distance of 16 R_E. This is interpreted to represent traversal of the magnetic neutral sheet in the earth's magnetic tail and is characteristic of observations of this phenomenon by IMP-I (Ness (42)).

15. Summary of the XY hourly component averaged measurements in 1964 by the IMP-I satellite while imbedded within the earth's magnetic tail. The lower portion of the figure corresponds to measurements performed while the satellite was more than 2.5 R_E below the ecliptic plane while the upper portion of the figure corresponds to positions of the satellite above this. Clearly evident

is the distortion of the geomagnetic field forming the extended geomagnetic tail (Ness (42)).

16. Schematic illustration summarizing the results of the IMP-I magnetic field experiment projected on the ecliptic plane from November 27, 1963 through May 31, 1964. The direction of the interplanetary magnetic field is observed to be approximately 45^{o} to the directed flow of the solar wind. Indicated are the relative positions of the satellite during the six month period during which the measurements were performed (Ness (42)).

17. Comparison of worldwide magnetograms during sudden commencement geomagnetic storm which occurred on May 10, 1964 at 0035 UT with magnetic field measurements by IMP-I satellite in the earth's magnetic tail. Evident is the simultaneous world wide increase at the onset of the storm correlated positively with an increase in field strength at a distance halfway to the moon. The subsequent main phase decrease is shown to be accompanied by an additional increase in tail field magnitude (Behannon and Ness (46)).

18. Correlation of magnetic tail measurements during the geomagnetic storm of April 1, 1964 with measurements of the trapped radiation boundary obtained by satellite 1963-38C (Ness and Williams, (48)). The invariant trapping boundary (Λ) is theoretically predicted by invoking a tail field model of the geomagnetic field

and is compared directly with observations (a to d). Also included is the planetary magnetic activity index Kp showing a positive correlation with tail field magnitude.

19. Photograph of comet Whipple-Fedtke-Tevzadze (1943I) indicating screwlike motions in the tail. Similarity of solar wind interaction with the geomagnetic field and with the cometary coma suggest that the earth may be compared to a "magnetic comet" with the magnetic tail and sheet corresponding to the observable ion-tail in the comet and the magnetosphere corresponding to the coma. (Photograph by C. Hoffmeister, Sonneberg).

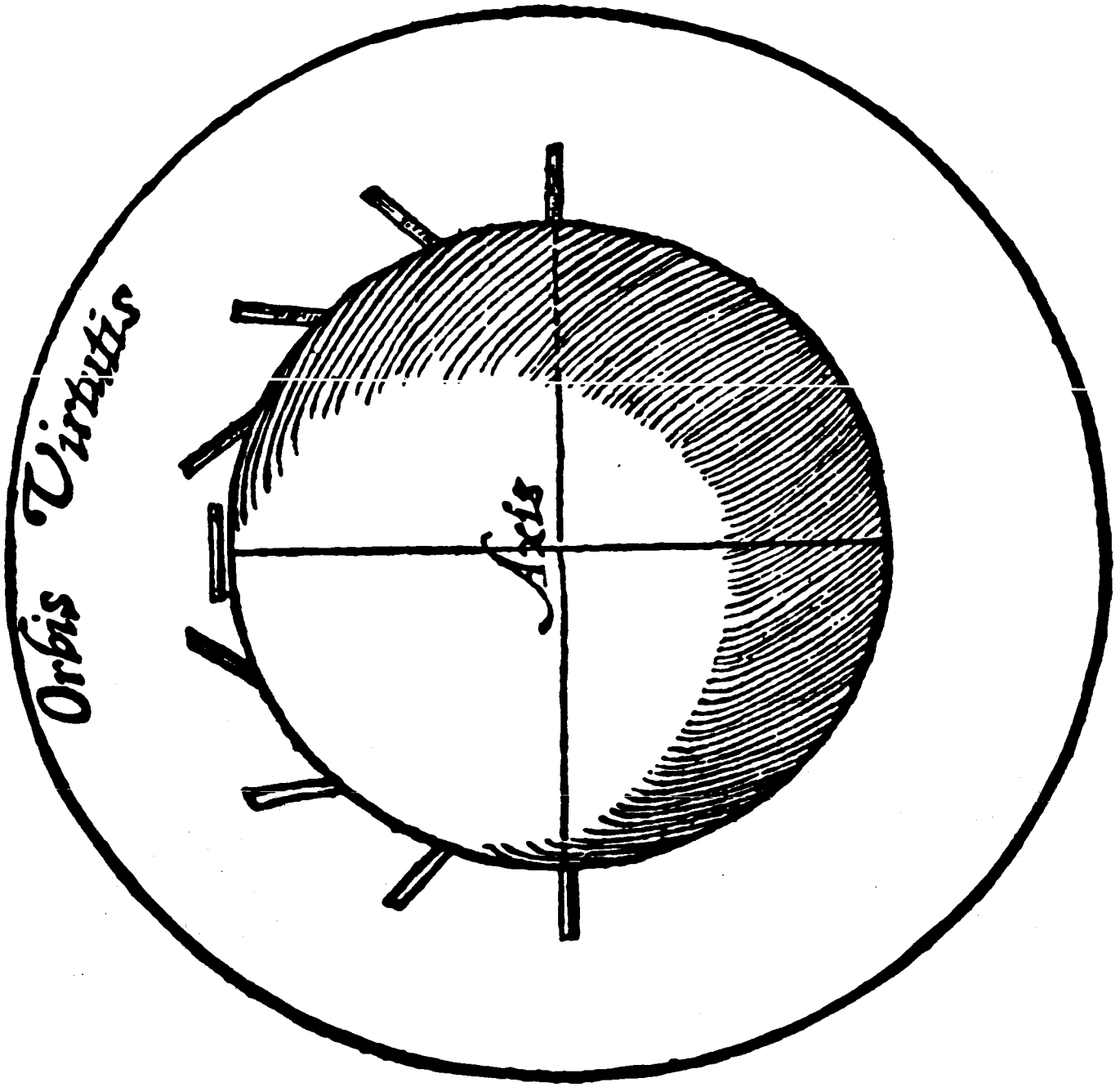

Figure 1

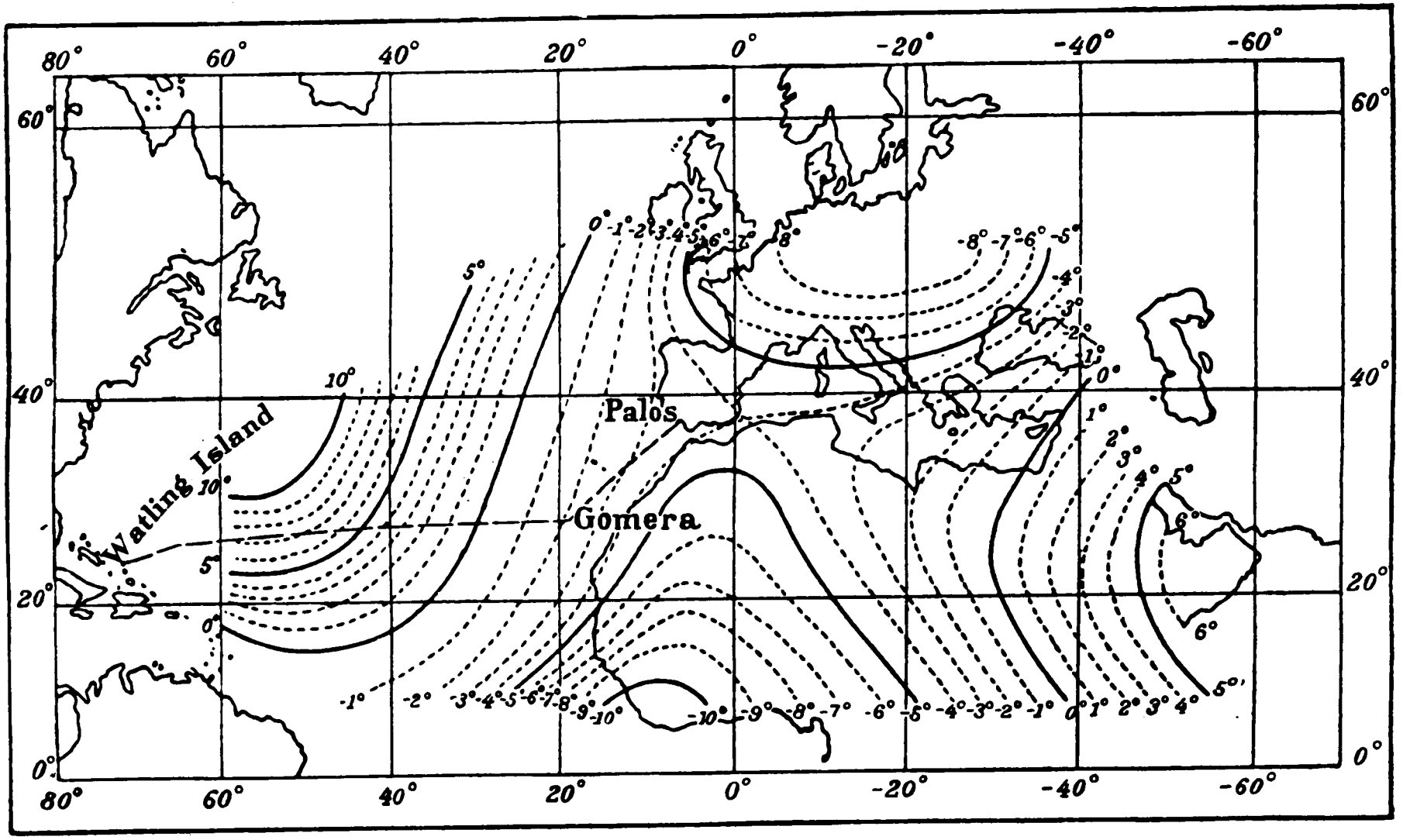

Figure 2

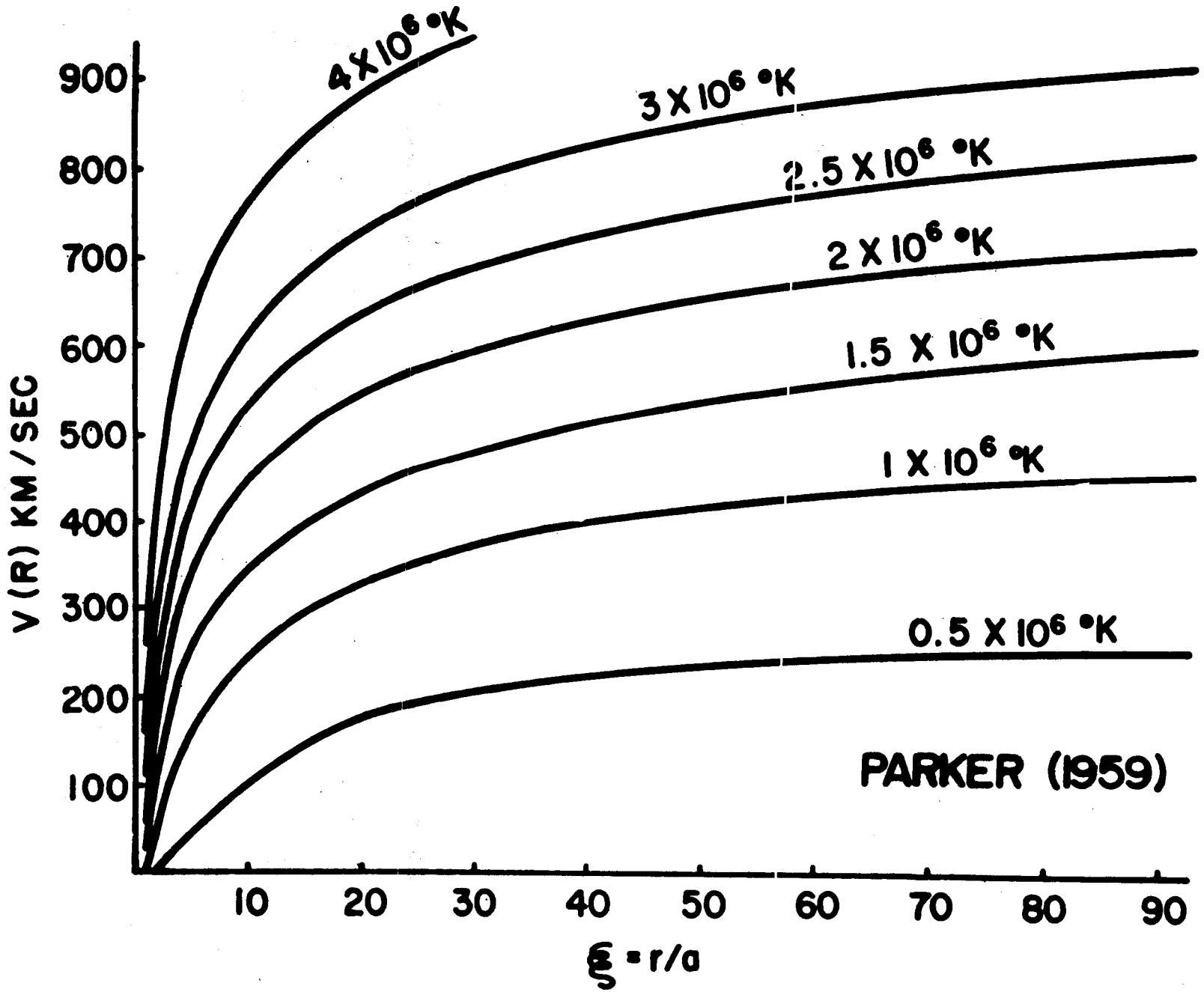
4 X 10^6 °K
3 X 10^6 °K
2.5 X 10^6 °K
2 X 10^6 °K
1.5 X 10^6 °K
1 X 10^6 °K
0.5 X 10^6 °K
PARKER (1959)
V(R) KM/SEC
900
800
700
600
500
400
300
200
100
10
20
30
40
50
60
70
80
90
ξ = r/a

Figure 3

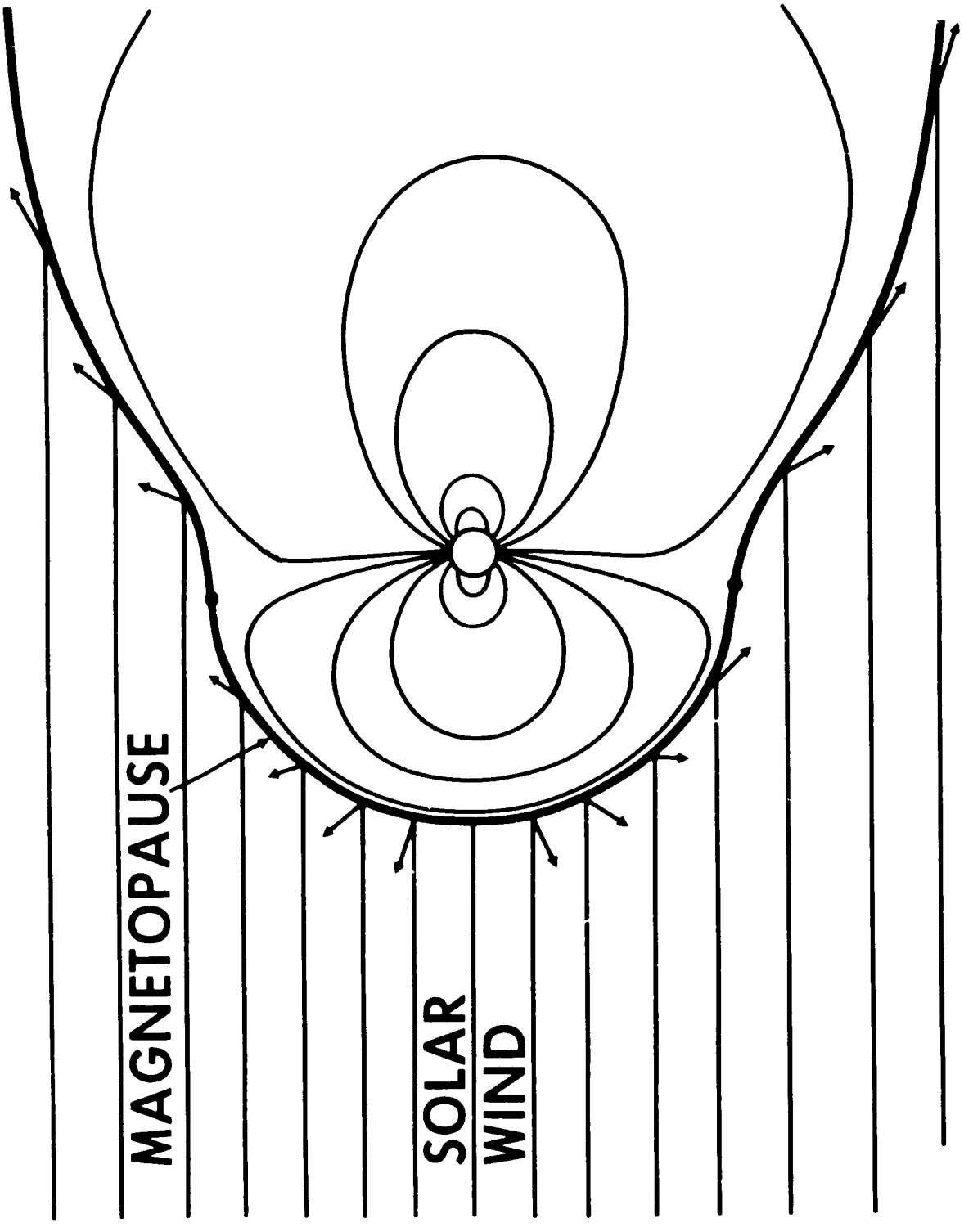

Figure 4

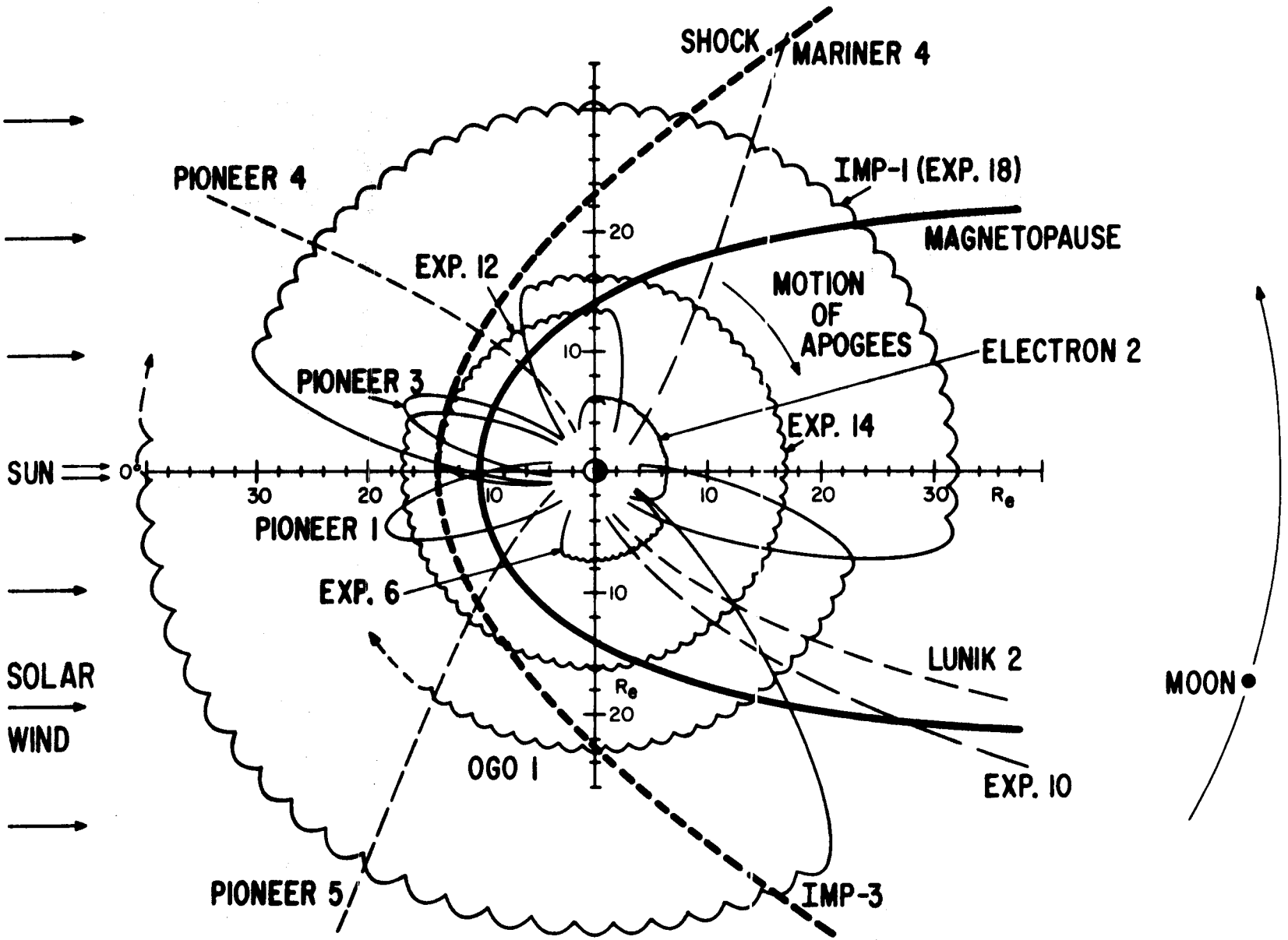
SHOCK
MARINER 4
PIONEER 4
IMP-1 (EXP. 18)
MAGNETOPAUSE
EXP. 12
MOTION
OF
APOGEES
ELECTRON 2
PIONEER 3
EXP. 14
SUN
0°
30
20
10
10
20
30
R_e
PIONEER 1
EXP. 6
10
LUNIK 2
SOLAR
WIND
R_e
20
MOON
OGO 1
EXP. 10
PIONEER 5
IMP-3

Figure 5

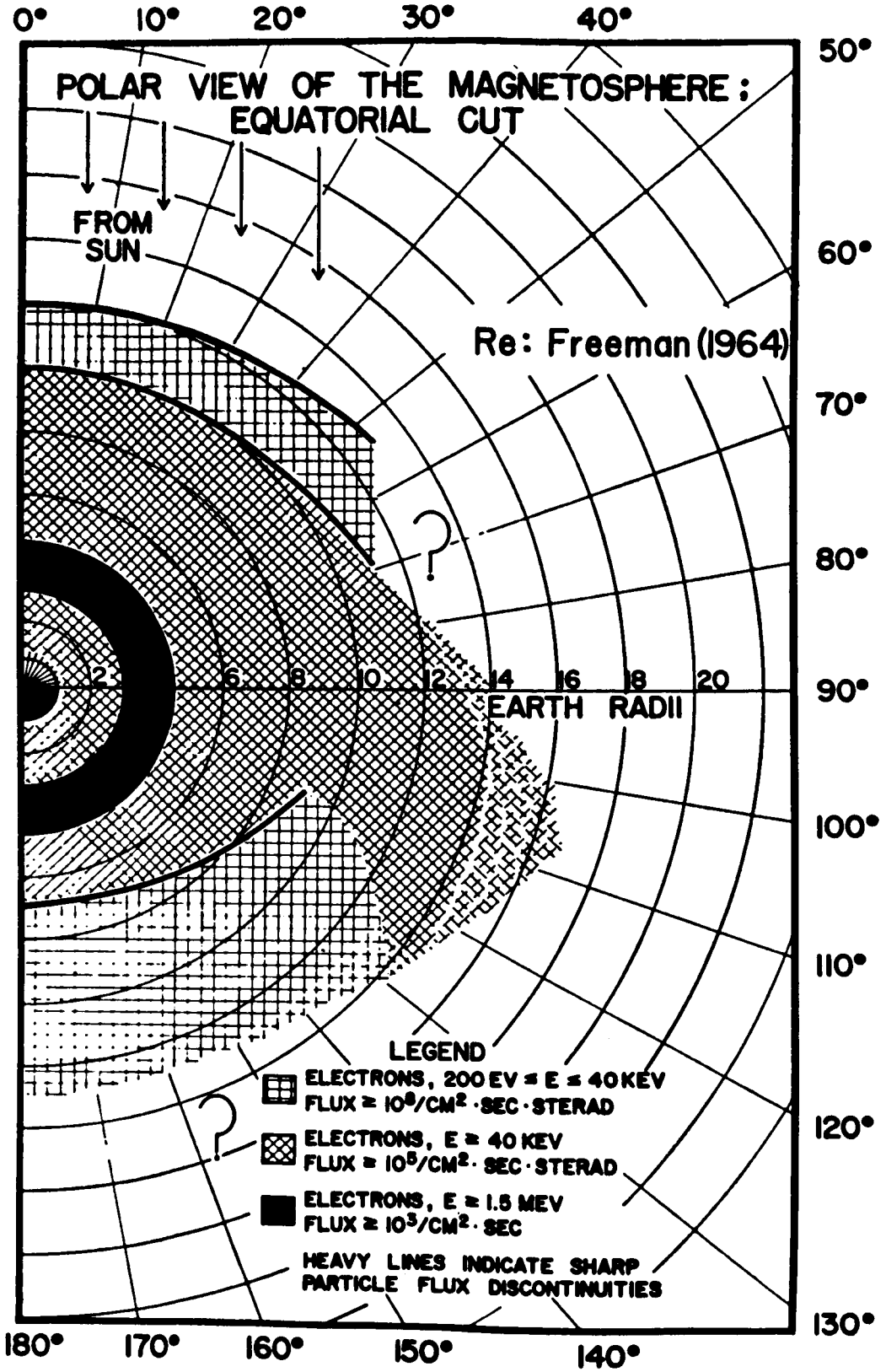
POLAR VIEW OF THE MAGNETOSPHERE:
EQUATORIAL CUT
FROM SUN
Re: Freeman (1964)
2
6
8
10
12
14
16
18
20
EARTH RADII
0°
10°
20°
30°
40°
50°
60°
70°
80°
90°
100°
110°
120°
130°
140°
150°
160°
170°
180°
LEGEND
ELECTRONS, 200 EV ≤ E ≤ 40 KEV
FLUX ≥ 10⁸/CM²·SEC·STERAD
ELECTRONS, E ≥ 40 KEV
FLUX ≥ 10⁵/CM²·SEC·STERAD
ELECTRONS, E ≥ 1.5 MEV
FLUX ≥ 10³/CM²·SEC
HEAVY LINES INDICATE SHARP
PARTICLE FLUX DISCONTINUITIES

Figure 6

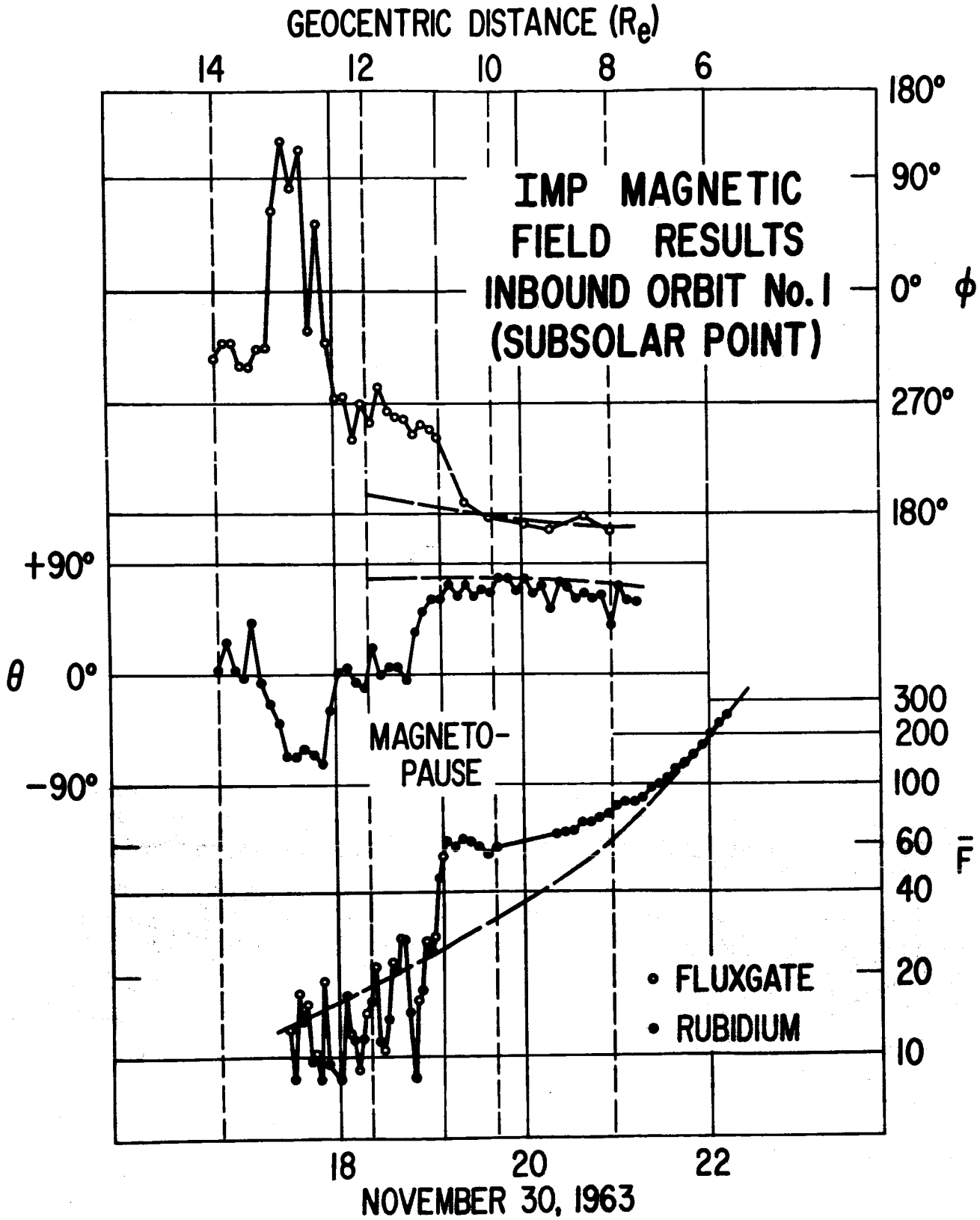
GEOCENTRIC DISTANCE (R_e)
14
12
10
8
6
IMP MAGNETIC FIELD RESULTS INBOUND ORBIT No. 1 (SUBSOLAR POINT)
180°
90°
0° φ
270°
180°
+90°
θ 0°
-90°
MAGNETO-PAUSE
300
200
100
60 F̄
40
20
10
• FLUXGATE
• RUBIDIUM
18
20
22
NOVEMBER 30, 1963

Figure 7

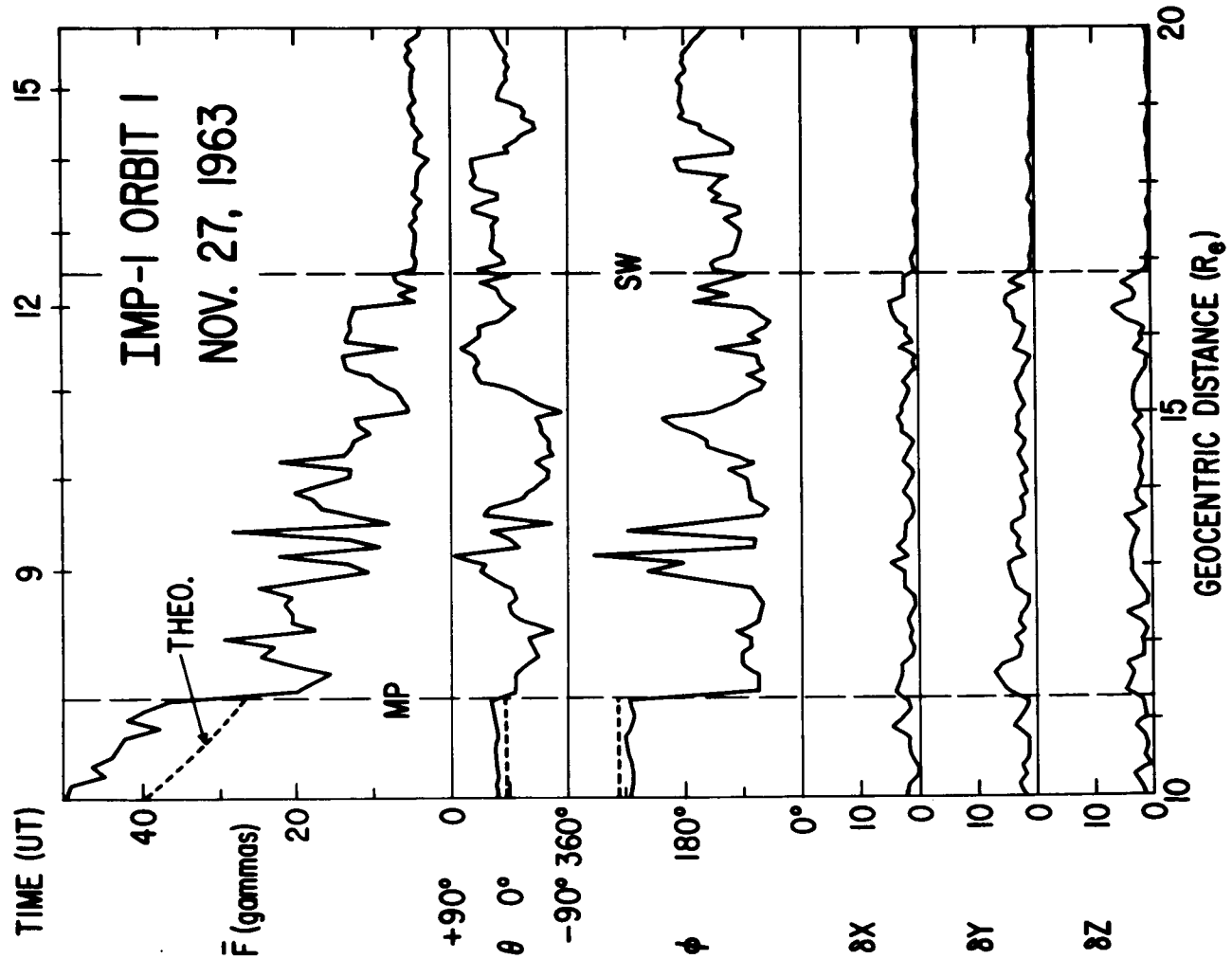
IMP-I ORBIT I
NOV. 27, 1963
TIME (UT)
9
12
15
40
20
F̄ (gammas)
THEO.
MP
SW
+90°
θ 0°
-90°
360°
0
180°
φ
0°
10
0
δX
δY
δZ
10
15
20
GEOCENTRIC DISTANCE (Re)

Figure 8

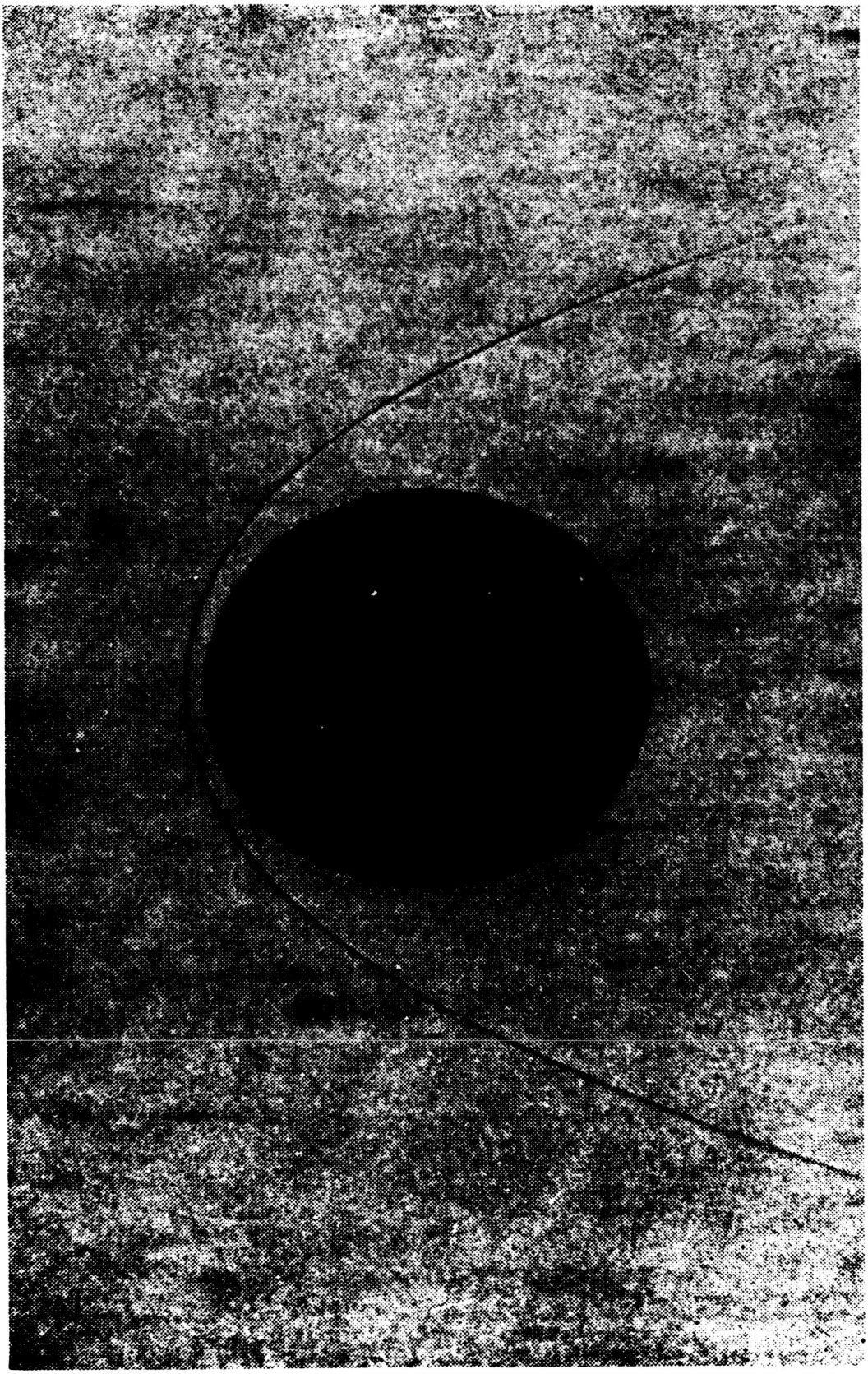

Figure 9

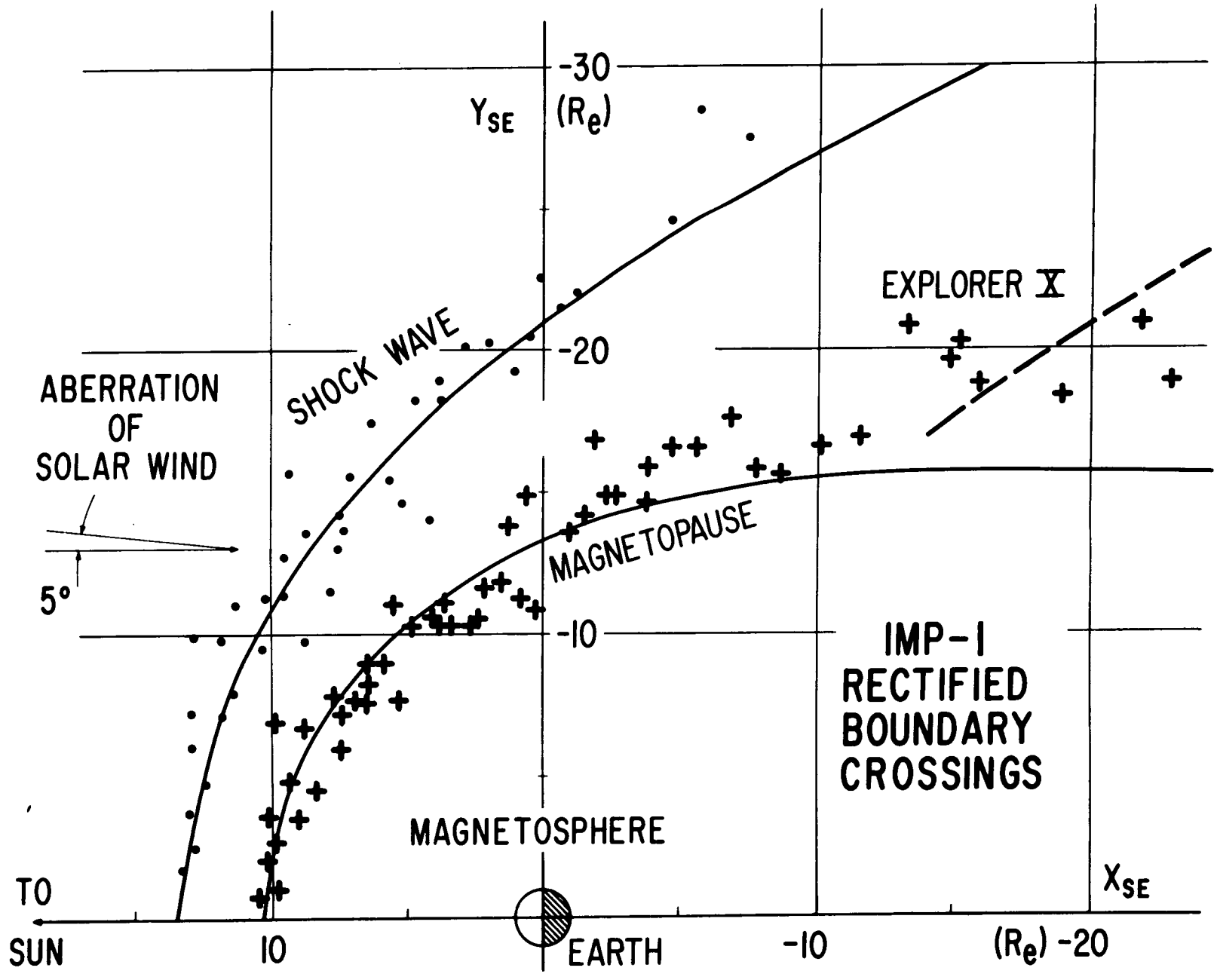
-30
Y_{SE} (R_e)
-20
-10
EXPLORER X
SHOCK WAVE
ABERRATION
OF
SOLAR WIND
5°
MAGNETOPAUSE
IMP-I
RECTIFIED
BOUNDARY
CROSSINGS
MAGNETOSPHERE
TO
SUN
10
EARTH
-10
(R_e) -20
X_{SE}

Figure 10

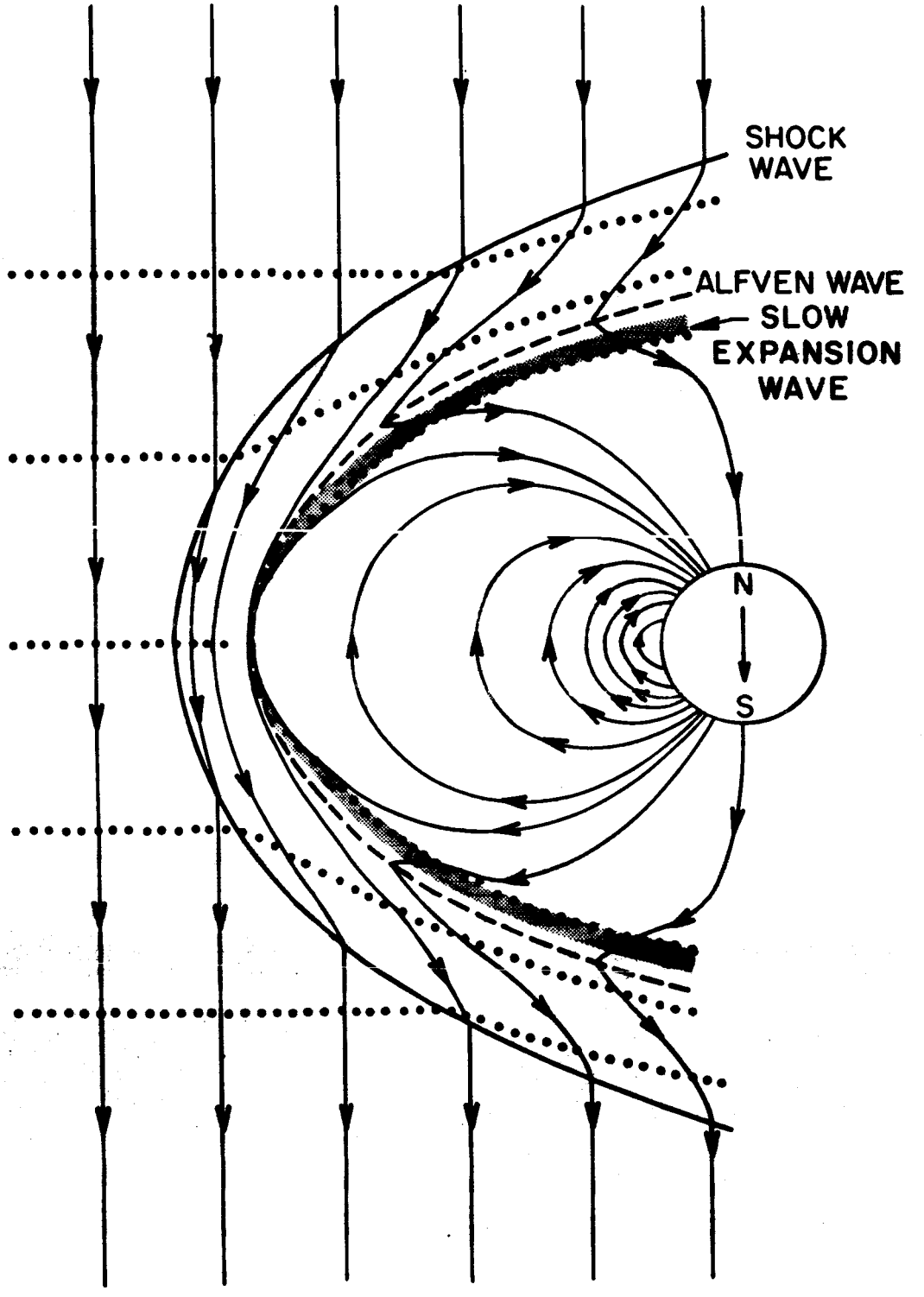

AFTER LEVY ET. AL. (1964)

Figure 11

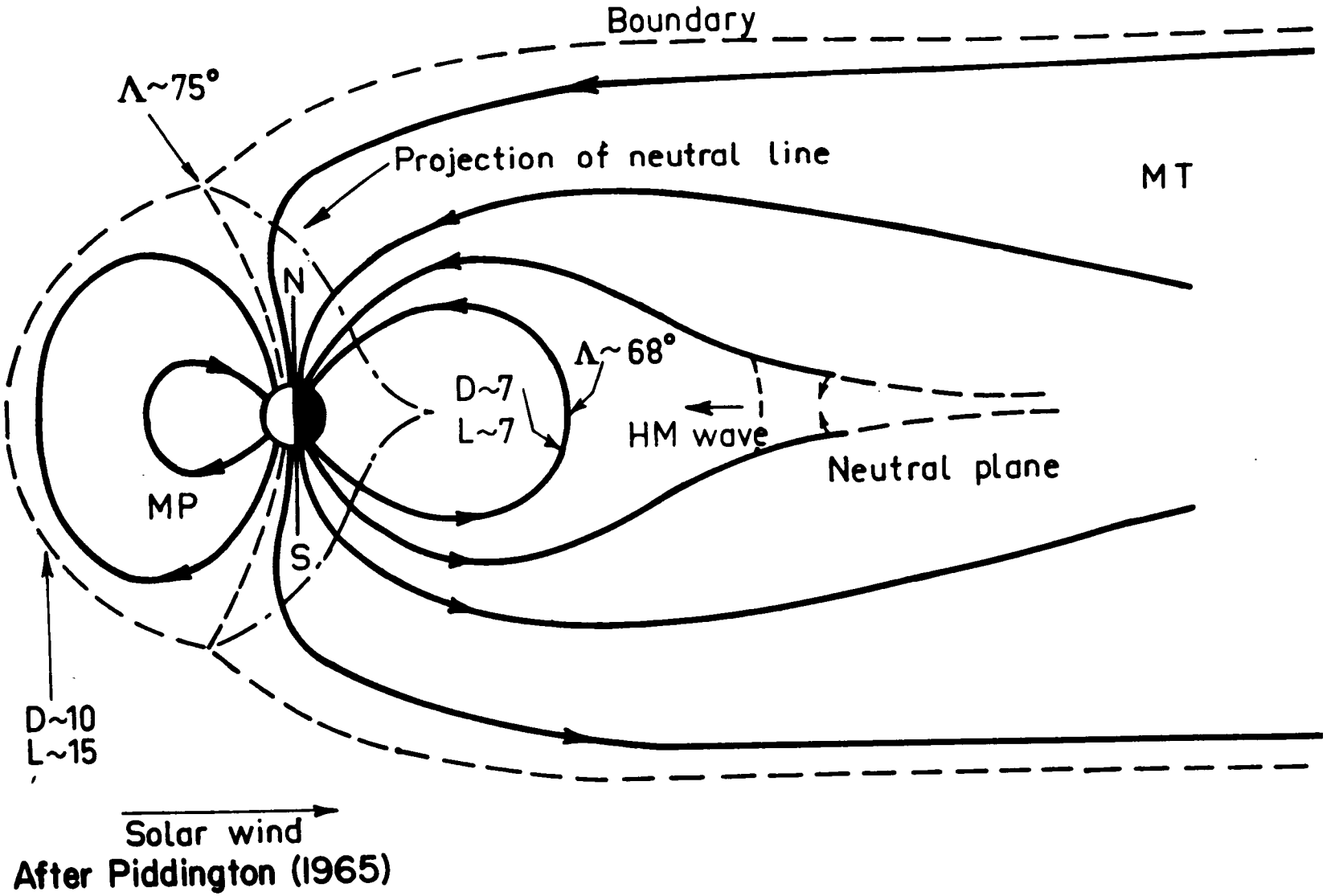

After Piddington (1965)

Figure 12

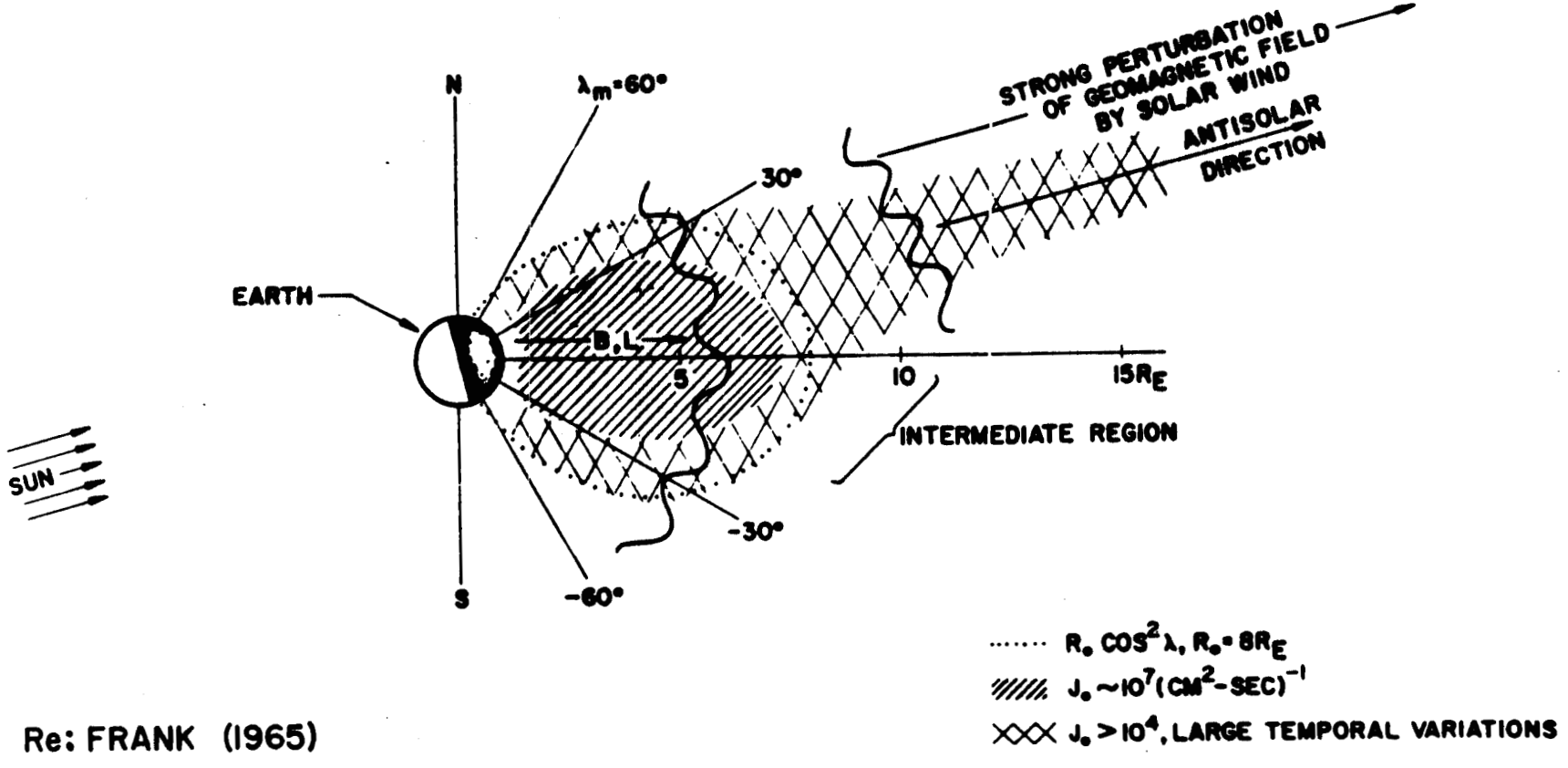

Figure 13

Re: FRANK (1965)

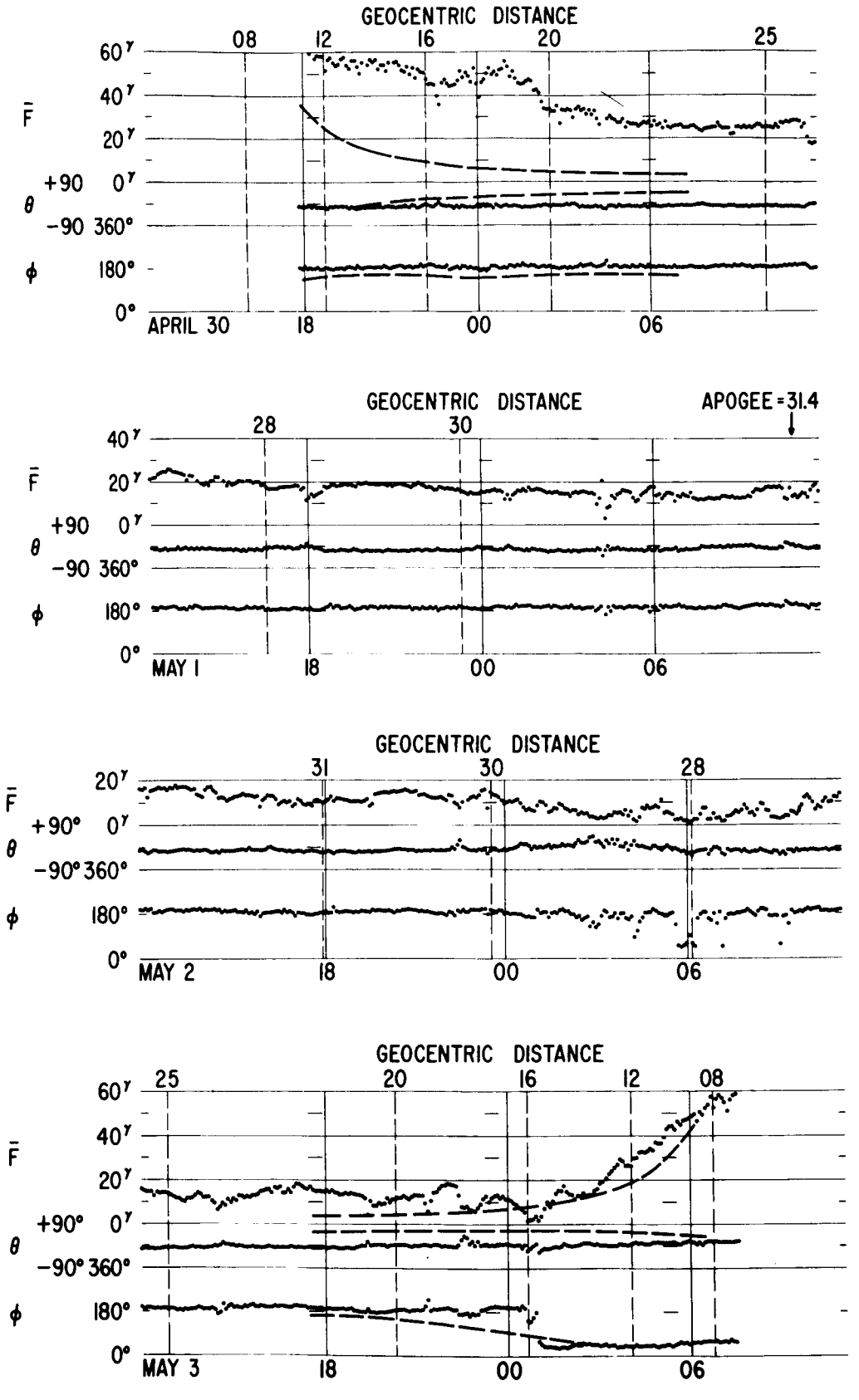

ORBIT NO. 41 IMP-I 1964

Figure 14

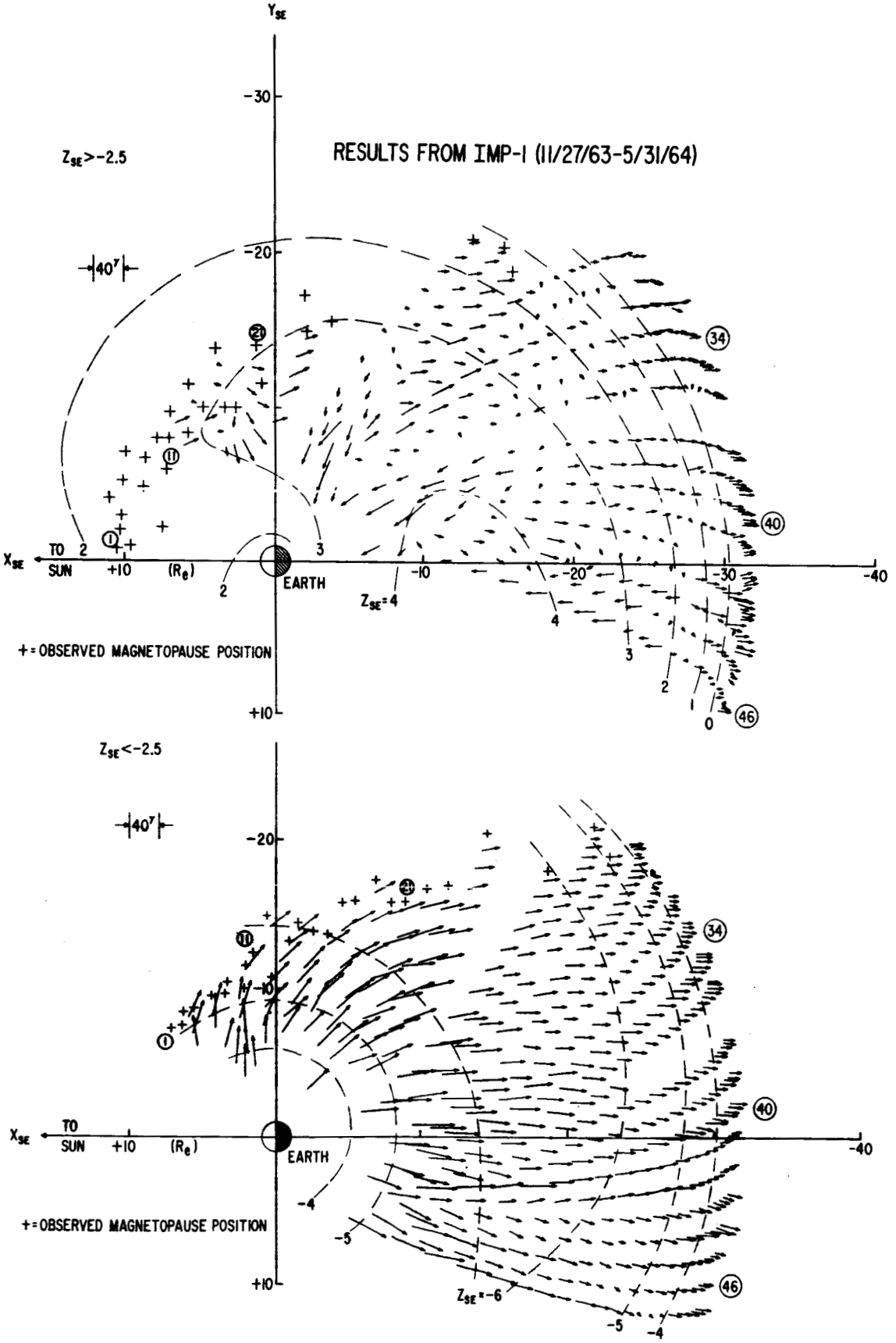
RESULTS FROM IMP-I (11/27/63-5/31/64)
Y_{SE}
Z_{SE}>-2.5
40γ
-30
-20
-10
+10
X_{SE}
TO SUN
+10 (R_e)
EARTH
-10
-20
-30
-40
Z_{SE}=4
+=OBSERVED MAGNETOPAUSE POSITION
Z_{SE}<-2.5
Z_{SE}=-6

Figure 15

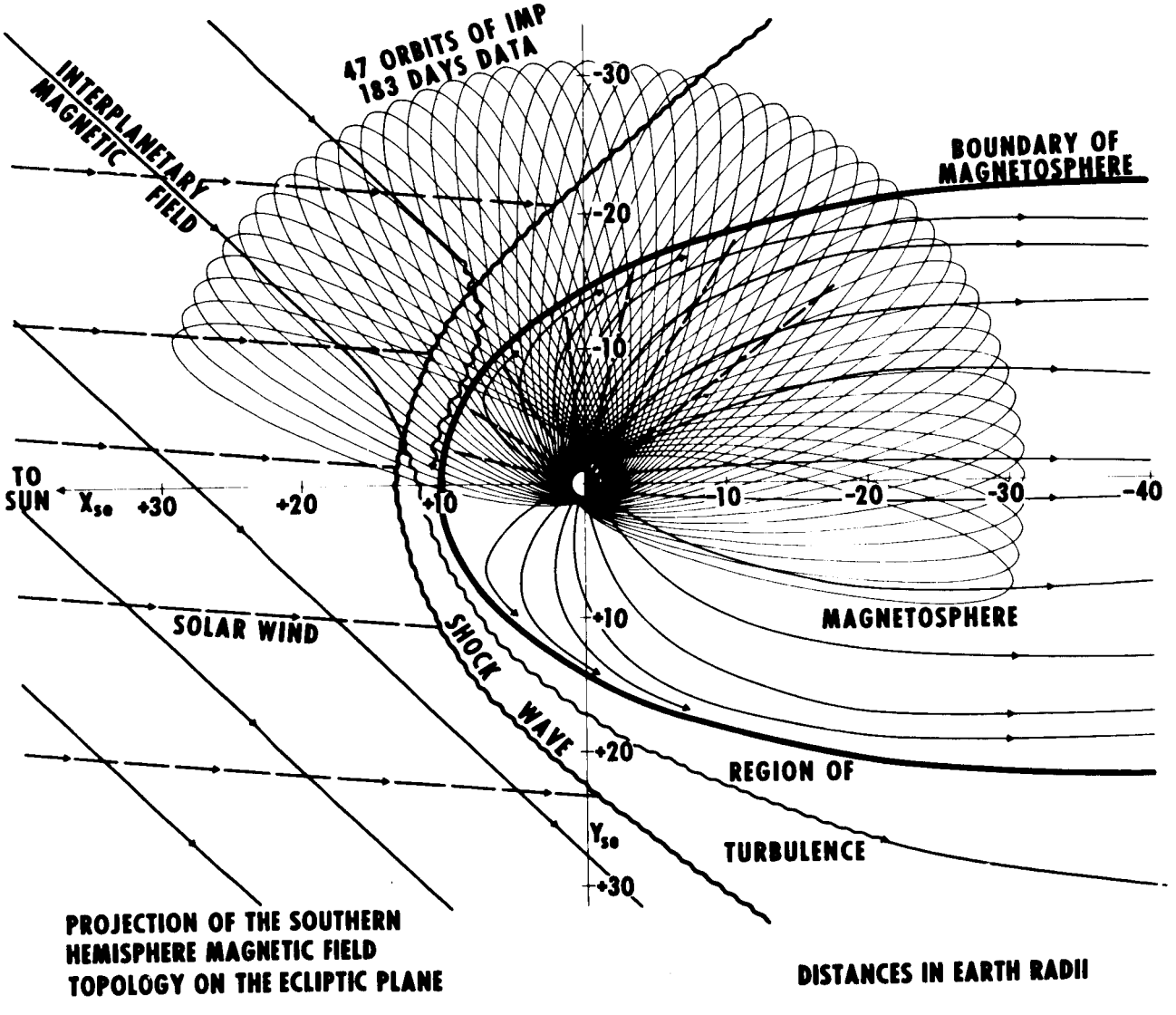
47 ORBITS OF IMP
183 DAYS DATA
INTERPLANETARY
MAGNETIC
FIELD
BOUNDARY OF
MAGNETOSPHERE
-30
-20
-10
TO
SUN
X_{se}
+30
+20
+10
-10
-20
-30
-40
SOLAR WIND
SHOCK WAVE
+10
MAGNETOSPHERE
+20
REGION OF
TURBULENCE
Y_{se}
+30
PROJECTION OF THE SOUTHERN
HEMISPHERE MAGNETIC FIELD
TOPOLOGY ON THE ECLIPTIC PLANE
DISTANCES IN EARTH RADII

Figure 16

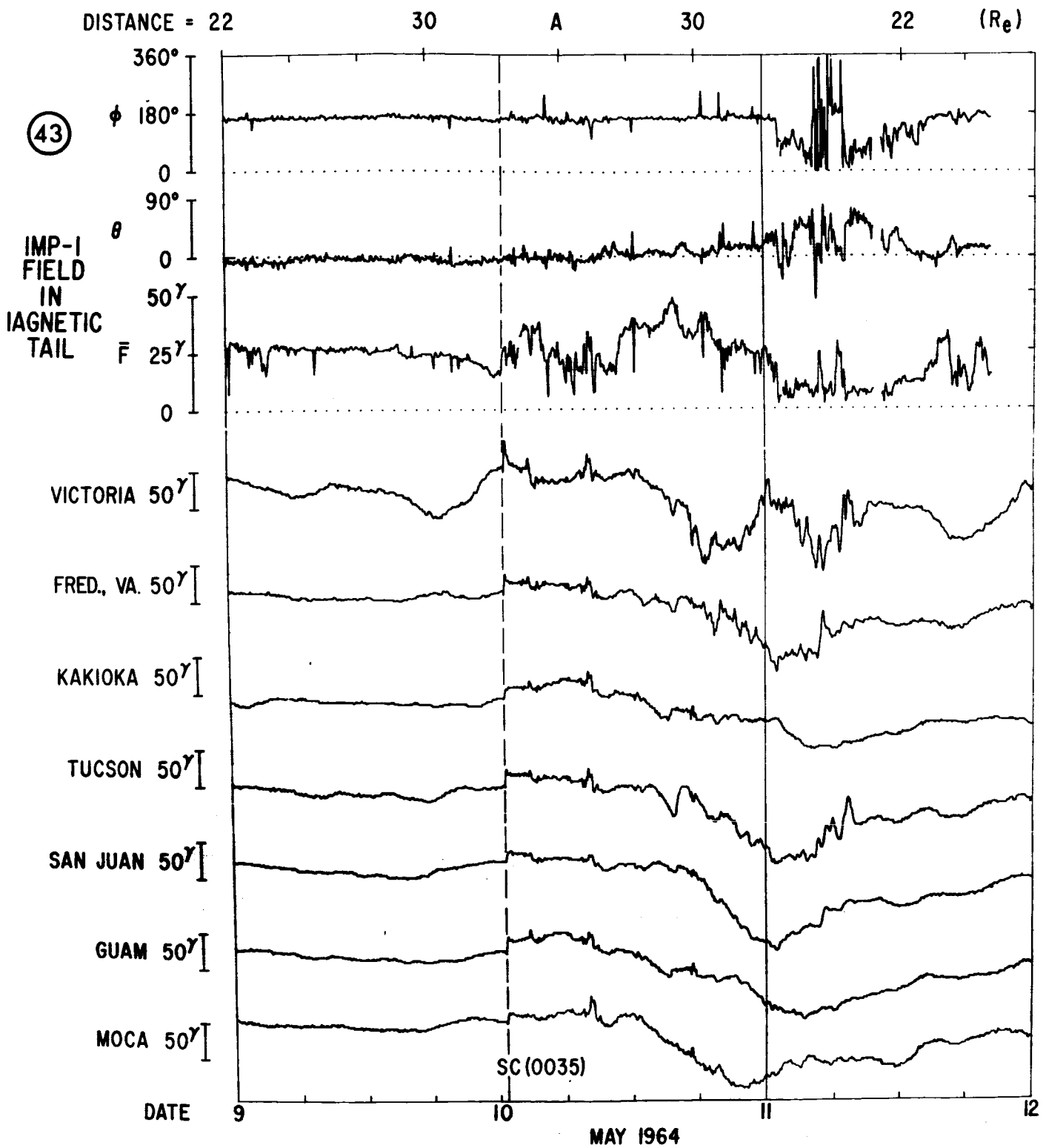
DISTANCE = 22
30
A
30
22
(Re)
360°
φ 180°
0
(43)
90°
θ
0
IMP-I
FIELD
IN
IAGNETIC
TAIL
50γ
F̄ 25γ
0
VICTORIA 50γ
FRED., VA. 50γ
KAKIOKA 50γ
TUCSON 50γ
SAN JUAN 50γ
GUAM 50γ
MOCA 50γ
SC (0035)
DATE
9
10
11
12
MAY 1964

Figure 17

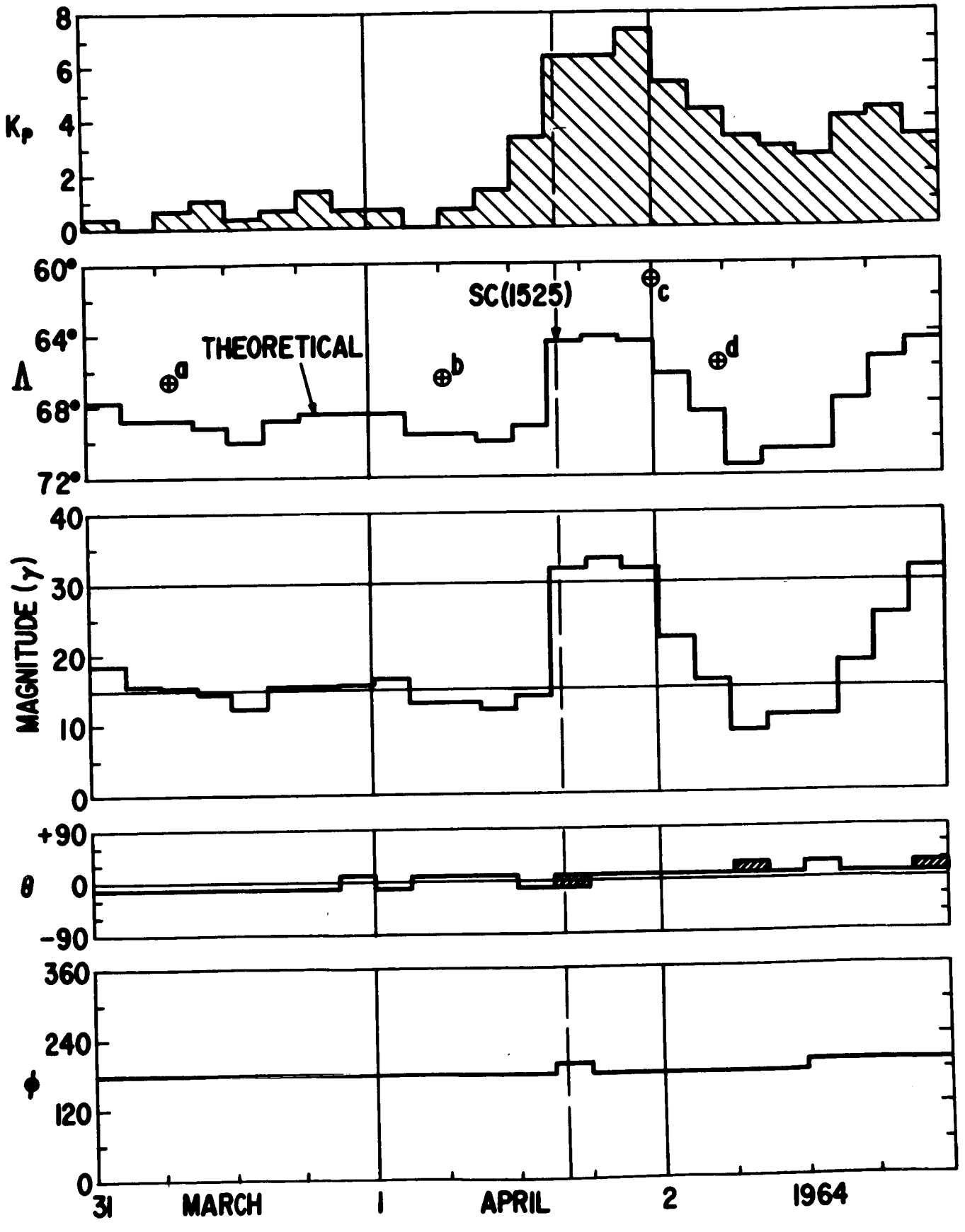
8
6
4
2
0
K_p
60°
64°
68°
72°
Λ
THEORETICAL
SC(1525)
a
b
c
d
40
30
20
10
0
MAGNITUDE (γ)
+90
0
-90
θ
360
240
120
0
φ
31
MARCH
1
APRIL
2
1964

Figure 18

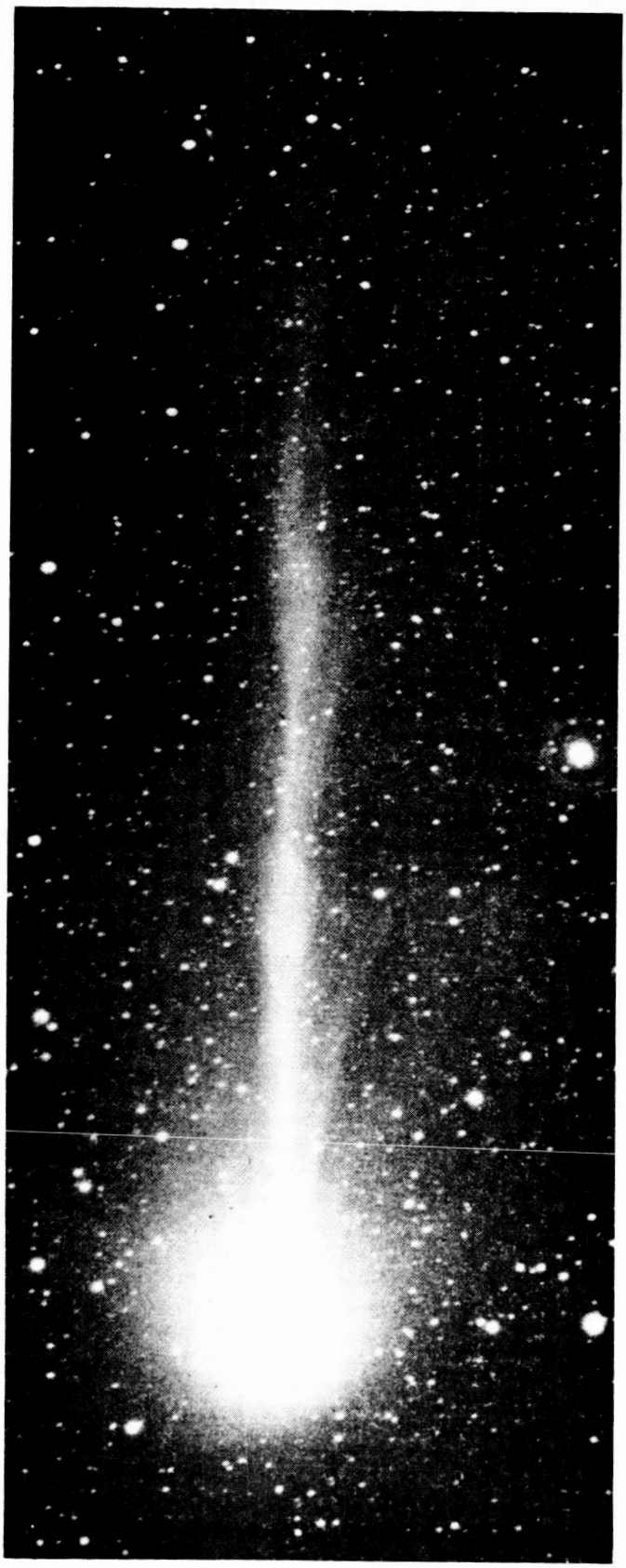

Figure 19

SATELLITE	LAUNCH	INCLINATION	LIFETIME (d)	RANGE (γ)	SENSITIVITY	DISTANCE (R_E)
SPUTNIK III	5-15-58	65°	30	$<6\times10^4$	5%	<1.3
PIONEER I	10-11-58	EARTH IMPACT	1	$<10^3$	1%	3.7-7.0 12.3-14.6
LUNIK I	1-2-59	SOLAR ORBIT	1	<6000	200γ	3-6
EXPLORER VI	8-7-59	47°	61	$<2\times10^4$	3%	2-7.5
LUNIK II	9-12-59	LUNAR IMPACT	33.5 HRS.	<1500	50γ	3-6
VANGUARD III	9-18-59	33°	85	10^4-6×10^4	4γ	<1.8
PIONEER V	3-11-60	SOLAR ORBIT	50	$<10^3$	0.05-5γ	5-9
EXPLORER X	3-25-61	33°	2.2	30 $\pm$ 50 — 5×10^3	3γ 0.3γ	1.8-7 6-42.6
EXPLORER XII	8-16-61	33°	112	$\pm$ 500	10γ	4-13.5
EXPLORER XIV	10-3-62	33°	300	$\pm$ 250	5γ	5-16.5
ALOUETTE	9-29-62	80°	STILL TRANS.	$<6\times10^4$	0.3%	1.17
EXPLORER XV	10-27-62	18°	90	$\pm$ 4000	40γ	1.7-4.0
EXPLORER XVIII (IMP-1)	11-27-63	33°	181	<300 <40	$\pm$0.25	<32
ELECTRON-2	1-30-64	61°	90	<120 <1200	2γ 20γ	3-11.6
COSMOS 26	3-18-64	49°	194	$<7\times10^4$	$\pm$4γ	~1.05
ELECTRON-4	7-11-64	61°	?	<240 <1200	?	3-11.4
OGO-A	9-5-64	31°	STILL OPER	<500	$\pm$3γ	3.8-24.3
EXPLORER-21 (IMP-2)	10-4-64	34°	150	<300 <40	$\pm$0.25γ	6-15.9

SATELLITE	LAUNCH	INCLINATION	LIFETIME (d)	RANGE	SENSITIVITY	DISTANCE
COSMOS-49	10-24-64	49^{o}	?	$<7 \times 10^{4}$	$\pm$ 4γ	~1.05
MARINER IV	11-28-64	SOLAR ORBIT	270	<370	$\pm$0.7γ	> 10
EXPLORER -26	12-21-64	20^{o}	STILL OPER.	$<2 \times 10^{3}$	$\pm$ 2γ	2.5-5.1
EXPLORER - 27 (IMP-3)	5-29-65	33^{o}	STILL OPER.	<300 <40	+0.25γ	<42

Table I Summary of US and USSR satellites and space probes launched since 1958 providing data on the geomagnetic field. Parameters represent inclination of orbital plane to equator, lifetime in days, dynamic range of instrumentation in gammas ($1\gamma = 10^{-5}$ oerstad = 10^{-5}), sensitivity (not accuracy) and the geocentric radial distance at which data was obtained.